29

Non-Thermal Effects of Near-Infrared Irradiation on Melanoma

Yohei Tanaka and Kiyoshi Matsuo
Department of Plastic and Reconstructive Surgery,
Shinshu University School of Medicine
Japan

1. Introduction

Malignant melanoma is considered to be the most aggressive form of skin neoplasms. Over the past few decades, the incidence rate of melanoma has steadily risen throughout the world.

The risks of developing melanoma consist of intrinsic and environmental factors. Intrinsic factors generally include a family history and an inherited genotype, while the most relevant environmental factor is sun exposure. Exposure to ultraviolet (UV) radiation is the most important environmental carcinogen (Travers et al., 2008) and plays a significant role in the development of melanoma (Wolf et al., 1994). Sunscreens reduce the effects of UV radiation on human skin (Ananthaswamy et al., 1997). Nevertheless, sunscreens have failed to protect against an increase in UV radiation-induced melanomas (Wolf et al., 1994).

Various kinds of UV blocking materials, such as sunblocks, films, paints, and fibers are often used to prevent skin damage from UV exposure. Although individuals all over the world use various kinds of sunscreens, unwanted biological influences such as rosasea, erythema ab igne, long-term vasodilation, muscle thinning, and sagging still occur (Tanaka et al., 2010c).

Most sunscreens can only block UV and not visible light or near-infrared (NIR) radiation. Sunlight that reaches the human skin contains solar energy composed of 6.8% UV light, 38.9% visible light, and 54.3% infrared (IR) radiation (Kochevar et al., 1999). In addition to natural NIR, human skin is increasingly exposed to artificial NIR from medical devices and from electrical appliances (Schieke et al., 2003; Schroeder et al., 2008). Thus, we are exposed to tremendous amounts of NIR.

Both UV and visible light radiation are attenuated by melanin (Anderson & Parrish, 1981), whereas NIR can penetrate deep into human tissue where it can cause photochemical changes (Karu, 1999). We previously reported that NIR penetrates the skin and is absorbed by sweat on the skin surface, water in the dermis (Tanaka et al. 2009a, 2009b), hemoglobin in dilated vessels (Tanaka et al., 2009b, 2011c), myoglobin in the superficial muscle (Tanaka et al., 2010c), bone cortical mass, and is scattered by adipose cells (Tanaka et al., 2011b). NIR irradiation induces strand breaks and cell death by apoptosis (Tirlapur & König, 2001) as well as the cell death of cancer cells and bone marrow cells (Tanaka et al., 2010b, 2011b). In addition, NIR irradiation is used as a therapeutic option for the treatment of wound healing

disorders (Danno et al., 2001; Horwitz et al., 1999; Schramm et al., 2003) and malignant tumors (Bäumler et al., 1999; Kelleher et al., 1999; Dees et al., 2002; Orenstein et al., 1999).

Despite the widespread therapeutic potential of NIR, the mechanisms responsible for the therapeutic actions of photobiomodulation with NIR have not been elucidated in detail. However, we found that NIR induced muscle thinning (Tanaka et al., 2010c, 2011a), bone marrow damage (Tanaka et al., 2011b), and had a cytocidal effect on cancer cells, which is likely due to apoptosis (Tanaka et al., 2010b).

NIR is easily absorbed by water, since water molecules are resonated by NIR due to the O-H intramolecular hydrogen bonds and electrical dipole moment (Tsai et al., 2001). NIR increases the amount of water retained in the dermis by inducing vasodilation and the expression of collagen, elastin, and water-binding proteins (Tanaka et al., 2009b). The NIR spectrum of biological materials results from the overtones and combination of O-H, C-H, and N-H groups' bond stretching vibrations (Weyer, 1985). Both collagen and elastin possess helical structures and hydrogen bonds. Elastin has higher absorption properties than water (Tsai et al., 2001). These findings suggest that we have acquired biological defense mechanisms in which induced helical structures and hydrogen bonds are resonated by NIR and absorb NIR to protect the subcutaneous tissues from this type of radiation.

NIR is also absorbed by choromophores, such as hemoglobin, or myoglobin, which have many alpha helices (Ferrari et al., 2004; Nancini et al., 1994). Alpha helices are thought to be resonated by NIR and have strong amide bands in the infrared spectra, which have characteristic frequencies and intensities (Nevskaya & Chirgadze, 1976). This implies that NIR induces the resonance of alpha helices in the oxygen-carrying proteins as well as the degeneration of proteins containing alpha helices, which results in damage to the storage and transport of oxygen, and therefore may be one of the mechanisms of apoptosis.

Nuclear lamins also have a central alpha helical structure (Prokocimer et al., 2009). Alpha helical structures of nuclear lamins are surmised to absorb NIR and protect the nucleus and DNA from NIR. NIR exposure appears to damage nuclear lamins and induce DNA damage. Nuclear lamina is transiently disassembled during mitosis (Gerace & Blobel, 1980; Nigg, 1992; Yang et al., 1997). In addition, actively proliferating cells show increased sensitivity to NIR (Karu et al., 1994; Tafur & Milles, 2008), and IR irradiation induces DNA strand breaks and apoptosis (Tirlapur & König, 2001). Therefore, these findings suggest that lamins may absorb NIR to protect the nucleus. Moreover, NIR may damage DNA of cells in the mitotic phase due to the absence of nuclear lamin protection, resulting in apoptotic cell death.

Thus, NIR irradiation has a potential application for transient mass reduction of proliferative malignant cancer, such as breast cancer and melanoma before surgery (Tanaka et al., 2010b), or for the treatment for terminal patients.

Continuous NIR exposure may damage lamins and induce mutations in the nuclear lamina genes. Alterations of nuclear lamins could also be involved in common disease processess, such as cancer (Foster et al., 2010), and may differentiate cancer cells from normal cells (Prokocimer et al., 2009). Skin tumors in mice appeared faster after irradiation with a full lamp spectrum containing UV, visible, and NIR compared to irradiation with UV alone (Bain et al., 1943). NIR irradiation may also induce carcinogenesis (Schieke et al., 2003) and enrich CD34-positive stem cells (Tanaka et al., 2011b). In this study, the mechanism of tumor cell death induced by NIR appeared to differ from a standard apoptosis mechanism, because high levels of activated caspase-3 expression and single-stranded DNA (ssDNA)-positive cells appeared gradually after NIR irradiation. However, tumor shrinkage occurred

rapidly. Therefore, NIR may induce apoptosis of highly proliferative melanoma cells, stimulate stem cells, and then induce apoptosis of the cells which are unnecessary to promote the development of melanoma. This appears to be a part of the mechanism for the effects of NIR.

The necessity to protect cells from NIR in order to prevent tissue damage has not been well investigated. Many studies have proven the effects of sun and UV exposure on melanoma, but have not investigated the long-term effects of NIR exposure on human skin and skin cancers.

Persons with fair skin, multiple atypical nevi or dysplastic nevi, or born with giant congenital melanocytic nevi are at increased risk of melanoma (Bliss et al., 1995). Fair skin with sparse melanin and a thin dermis might allow NIR radiation to penetrate deeper into human tissue than dark skin, which has dense melanin and a thick dermis (Tanaka et al., 2010c). Thus, sunscreens should also protect against NIR (Pujol & Lecha, 1993; Schieke et al., 2003; Tanaka & Matsuo, 2008; Tanaka et al., 2010c, 2011b, 2011c). Our preliminary studies suggest that we should consider the effect of not only UV, but also NIR on melanoma. In this study, we present an overview of our current understanding of the biological effects of NIR radiation on melanoma through experimental studies.

2. Experimental part

2.1 NIR irradiation

2.1.1 NIR device and wavelength

NIR irradiation was performed with a broadband infrared source (Titan; Cutera, Brisbane, CA, USA). The NIR device emits an NIR spectrum between 1100 to 1800 nm, with water filtering to remove wavelengths between 1400 and 1500 nm (Figure. 1), and simulates solar NIR radiation that reaches the skin of humans on the Earth's surface. This device delivers NIR without the wavelengths that are strongly absorbed by water and haemoglobin, which allow for the safe delivery of NIR energy deeper into tissue. The horizontal spot size of the irradiation was 10 × 30 mm.

To avoid thermal effects, the sapphire contact cooling tip was set to a fixed temperature of 20 °C to provide contact cooling. The sapphire block was cooled with fluids using thermoelectric coolers. Cooling fluids were circulated by a pump and a cooling system. Pre- and parallel-irradiational cooling of the superficial layers was accomplished using this temperature-controlled sapphire window, which further prevented excessive superficial heating.

These specific wavelengths and the cooling system enabled the delivery of NIR to deeper tissues without pain or epidermal burns.

2.1.2 NIR irradiation and output

We previously reported that 3 rounds of NIR irradiation consisting of 2 passes at 20 J/cm^2 was sufficient to induce histological changes in the epidermis of rats, but that higher energies had a greater response and were preferable to see effects in deeper tissues.

The correlation with efficacy seemed to be highest with total delivered energy, not per pulse fluence, since multiple irradiations with a lower output appeared as equally effective as higher fluence irradiations.

Therefore, we performed NIR irradiation at 40 J/cm2 for the *in vivo* study.

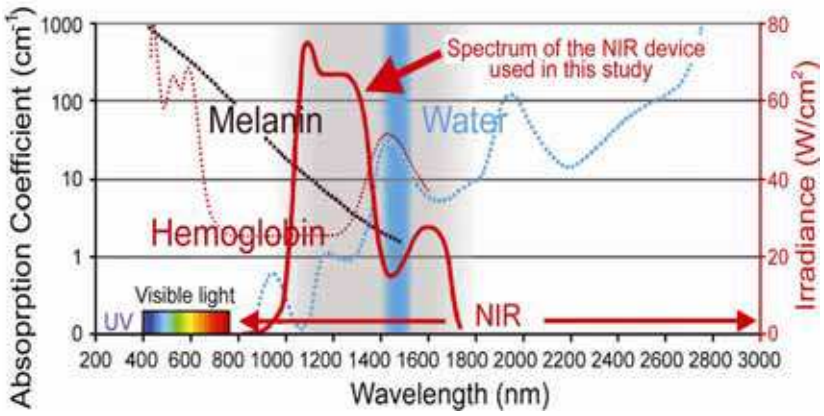

Fig. 1. The absorption coefficients and wavelength of the NIR device. This graph shows the absorption coefficients of melanin (brown), hemoglobin (red), and water (blue). The NIR device used in our study emits a spectrum of NIR from 1100 to 1800 nm (bold red), with filtering of wavelengths between 1400 and 1500 nm (blue belt) that are strongly absorbed by water and hemoglobin. These specific wavelengths and the cooling system enabled the delivery of NIR to deeper tissues without pain or epidermal burns. Cited and revised from Fig. 2. Tanaka et al. (2010). Long-lasting muscle thinning induced by infrared irradiation specialized with wavelength and contact cooling: A preliminary report. *ePlasty*. 10:e40

2.2 *In vitro* tumorigenicity and treatment

2.2.1 Cell culture

Testing was conducted on cultures of 2 melanoma cell lines: B16F0 melanoma cells and MDA-MB435 melanoma cells. B16F0 and MDA-MB435 melanoma cell lines were obtained from the American Type Culture Collection (ATCC, Manassas, VA, USA). B16F0 and MDA-MB435 cells were maintained in DMEM (Invitrogen, Carlsbad, CA, USA) medium supplemented with 10% fetal bovine serum and antibiotics. Cells were seeded in 96-well microtitre plates at a concentration of 5 x 10^3 cells per well in 100 µL of medium. All cells were grown at 37°C in a humidified incubator with 5% CO_2. A total of 768 wells of cancer cell lines were prepared for this study.

2.2.2 Cell culture and NIR irradiation

Cancer cells from the 2 melanoma cultures were divided based on the number of individual NIR exposures in a single session and the total irradiation received. The numbers of exposures performed per round were 3, 10, and 20 exposures using two separate fluence settings per exposure of 20 J/cm^2 and 40 J/cm^2, because our preliminary results indicated that 3 shots at 10 J/cm^2 on cultured cancer cells (B16F0 cells) were not effective. This resulted in 7 different groups (including the control group) for each of the 2 cancer cell lines. The irradiated groups were exposed to a single round of irradiation. The MTS assay was performed after a 3-day incubation period following the exposure session.

2.2.3 Cell proliferation assay

We performed an MTS cell proliferation assay to evaluate the effects of NIR irradiation. Cell proliferation was analyzed using a CellTiter 96 Aqueous Cell Proliferation Assay kit (Promega,

Madison, WI, USA). Aliquots of 20 µL of MTS reagent were added to the wells and incubated at 37°C in a humidified incubator for 2 hours. Absorbance at 490 nm (OD_{490}) was monitored with a Powerscan HT microplate reader (Dainippon Pharmaceutical, Osaka, Japan).

2.3 *In vivo* tumorigenicity and treatment

Animals were housed in a temperature-controlled environment under a 12-h light-dark cycle with free access to water and standard mouse chow. Body weight and tumor size were measured every other day. Tumor volumes were defined as 4/3 x π x (longest diameter)/2 x (shortest diameter)/2 x (shortest diameter)/2. This study was approved by the Shinshu University Institutional Review Board for Animal Study. In addition, national and international principles of laboratory animal care were followed throughout the study.

Forty female nude mice (Crlj:CD1-Foxn1nu) were obtained from Charles River Laboratories (Yokohama, JAPAN). MDA-MB435 cells (5.0 x 10^6 cell/100µL/mouse) were implanted subcutaneously in the right flank of 6-week-old mice. Twenty-eight mice were divided into two groups when the tumor volume expanded to approximately 100 mm^3. The mice were divided into groups 19 days after tumor transplantation, which was defined as day 1 for testing. Groups consisted of two equal groups (n = 14 for each group): one group (control group) was untreated, whereas the other group was treated with NIR irradiation. NIR irradiation was started on days 1 and 31. Treatments were performed once daily for 13 days. All treatments consisted of 10 exposures of IR irradiation at 40 J/cm^2. Animals were euthanized at 99 days after tumor transplantation (day 80).

2.3.1 Histological investigation

MDA-MB435 tumors were taken from nude mice on days 3 (n = 4), 9 (n = 4), 45 (n = 4), and 80 (n = 16) for histological examination. Specimens were fixed in 20% neutral buffered formalin and processed for paraffin embedding. MDA-MB435 tumors were serially sectioned in the vertical plane (3–4 μm thickness). Specimens were evaluated by hematoxylin and eosin (H&E) staining, transferase-mediated dUTP nick-end labeling (TUNEL) technique, and immunohistological staining using an anti-Ki67 antibody, caspase-3, and single-stranded DNA as readouts. The sections were photographed under an Olympus BX51 microscope (Olympus, Tokyo, Japan) equipped with a digital camera system (DP50; Olympus). The digital photographs were processed using Adobe Photoshop (Adobe, San Jose, CA, USA).

2.4 *In vivo* bone marrow assessment

Thirty-five male Wistar rats (*Rattus norvegicus albinus*) weighing 360 - 440 g were used. Thirty-five rats were either irradiated (n = 25) or not irradiated (control; n = 10). The centre of the dorsal portion of the irradiated rats was subjected to 3 rounds of irradiation at 40 J/cm^2 on days 0, 7, and 14 without application of topical anesthesia. One round of treatment consisted of two passes of NIR irradiation.

2.4.1 Histological investigation

Specimens, which included the spinous process of the sixth lumbar vertebra and the overlying subcutaneous tissues, were isolated from the experimental group (5 rats per time point) at 7, 30, 60, 90, and 180 d after the final -dose of irradiation (d7, d30, d60, d90, and d180, respectively). Control samples were only isolated at day 0 and day 180 (5 rats per time point).

The specimens were fixed in 20% neutral buffered formalin, paraffin embedded, and serially sectioned along the sagittal plane (3 - 4 μm thickness). Tissue sections were stained with H&E as well as with an anti-CD34 antibody for immunohistochemical analysis to detect CD34-positive hematopoietic stem cells in the bone marrow.
The percentage of the area occupied by bone marrow adipocytes, the number of hematopoietic bone marrow cells, and the number of CD34-positive stem cells were calculated in a superficial area 1.5 mm deep in the spinous process.
Images were scanned and quantified in 5 representative fields per section and subsequently averaged to obtain a final score. The sections were photographed under an Olympus BX51 microscope (Olympus, Tokyo, Japan) equipped with a digital camera system (DP50; Olympus). The digital photographs were processed using Adobe Photoshop (Adobe, San Jose, CA, USA).

2.5 Statistical analysis

The differences between groups at each time point were examined for statistical significance with a Student *t*-test for the melanoma studies and the Mann-Whitney U -test for the stem cell studies. $P < 0.05$ was considered to be statistically significanct.

3. Results

3.1 Cell viability measured by the MTS assay

The OD_{490} values of irradiated cell cultures decreased significantly compared to controls in both B16F0 and MDA-MB435 cell lines, except at the lowest dose of irradiation with three, 20 J/cm^2 exposures (group 20 J x 3) ($P < 0.001$) (Fig. 2).

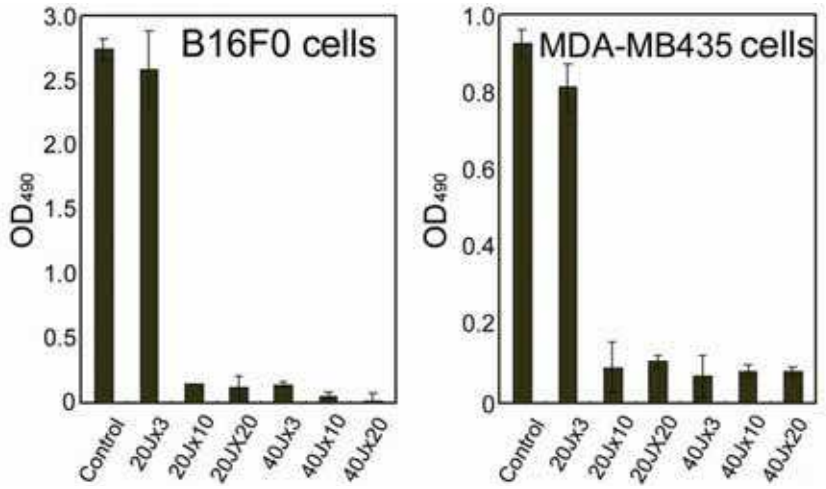

Fig. 2. The values of OD_{490} in B16F0 melanoma cells (left) and MDA-MB435 melanoma cells (right). The OD_{490} values of irradiated cell cultures, with the exception of the lowest NIR irradiation group of 3 exposures at 20 J/cm^2, decreased significantly ($P < 0.001$, compared to controls) in all cultures. Cited and revised from Fig. 2. Tanaka et al. (2010). Non-thermal cytocidal effect of infrared irradiation on cultured cancer cells using specialized device. *Cancer Science*. 101:1396-402

Group 20 J x 3 showed the smallest decrease in cell viability in MDA-MB435 cells that was still significant (P = 0.034), but only modest reductions were observed in B16F0 cells. No statistically significant intra-group differences were observed between the 20 and 40 J/cm^2 treatment groups (excluding group 20 J x 3). This was consistently observed for both cancer cell lines.

Ten exposures at 20 J/cm^2 achieved a comparable significant reduction in cell count as that of 3 exposures at 40 J/cm^2. Three exposures at 20 J/cm^2 appeared close to a threshold energy dosage.

3.2 *In vivo* tumor volume

Significant differences were observed in tumor volume between the control group and NIR irradiated group from day 5 up to day 77 (Fig. 3).

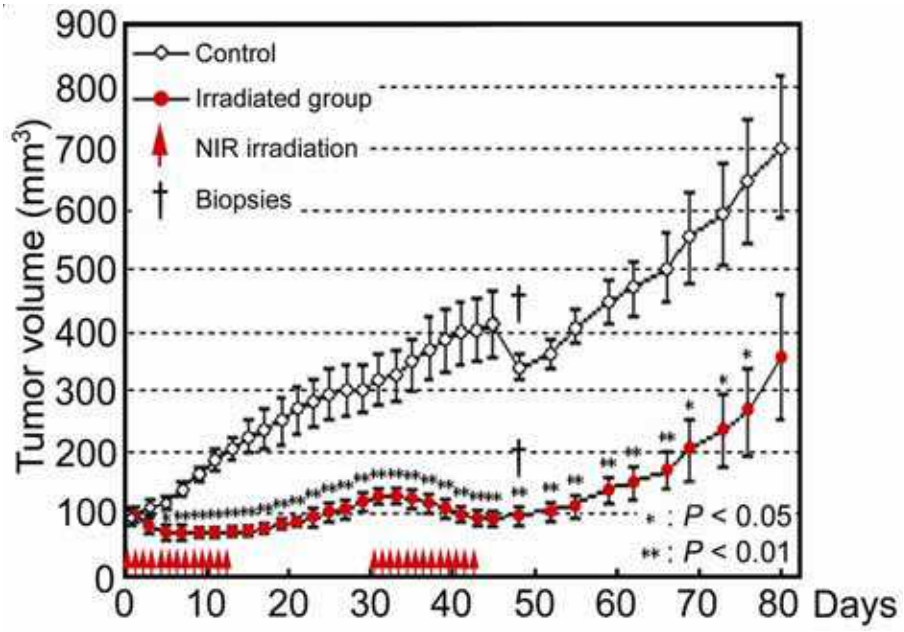

Fig. 3. Relative tumor volume of MDA-MB435. Significant differences were observed in tumor volume between the control group and NIR irradiated group from day 5 up to day 77. NIR irradiation was started on day 1 when the tumor volume expanded to approximately 100 mm^3, and then restarted on day 31. Treatments were performed once daily and all treatments consisted of 10 exposures of NIR irradiation at 40 J/cm^2. Significant differences were observed in MDA-MB435 tumor volume between the control group and NIR irradiated group from day 5 up to day 77. Significant differences are indicated (*: P < 0.05, **: P < 0.01). The cross sign indicates when two animals of each group were euthanized for histological investigation (day 45). Cited from Fig. 4. Tanaka et al. (2010). Non-thermal cytocidal effect of infrared irradiation on cultured cancer cells using specialized device. *Cancer Science*. 101:1396-402

The mean tumor volume of MDA-MB435 cells in the control group was 99.0 ± 26.85 mm^3 on day 1 of the treatment and increased continuously to 700.5 ± 333.8 mm^3 on day 80. The mean tumor volume for the irradiated MDA-MB435 group was 100.0 ± 26.06 mm^3 on day 1 of the treatment. Tumor volume decreased after the 1st round of IR irradiation and continued to reduce through day 5 to a minimum volume of 67.0 ± 15.75 mm^3. After day 5, the mean tumor volume gradually increased in the irradiated group through day 15, resulting in a tumor volume of 129.0 ± 44.05 mm^3 on day 31 when the second treatment started. Following the second round of irradiation, the mean tumor volume again decreased, reducing the tumor volume to 94.0 ± 41.22 mm^3 by day 45. Subsequently, the mean tumor volume began to increase gradually and reached 357.3 ± 297.2 mm^3 by day 80.

3.2.1 Histology of transplanted melanoma

The histology of the irradiated groups showed tumor shrinkage in MDA-MB435 cells (Figures 4-6). Injured cells were observed in the vertical histological section of NIR irradiated MDA-MB435 melanoma tumors on day 45 (Figure 4).

Significant differences between the control and irradiated groups were observed in the frequencies of Ki67-positive and TUNEL-positive on day 9 as well as caspase-3-positive and ssDNA-positive cells on day 45 ($P < 0.05$) (Figure. 8). The frequencies of Ki67-positive cells in the control group and irradiated group on day 9 were 13.82 ± 6.53% and 0.76 ± 0.12%, respectively. The frequencies of Ki67-positive cells in the control group and irradiated group on day 45 were 35.22 ± 16.10% and 31.78 ± 3.48%, respectively.

The frequencies of TUNEL-positive cells in the control group and irradiated group on day 9 were 0.84 ± 0.47% and 3.71 ± 2.22%, respectively. The frequencies of TUNEL-positive cells in the control group and irradiated group on day 45 were 1.09 ± 0.44% and 18.58 ± 21.48%, respectively. The frequencies of caspase-3-positive cells in the control group and irradiated group on day 9 were 0.36 ± 0.22% and 1.60 ± 0.86%, respectively. The frequencies of caspase-3-positive cells in the control group and irradiated group on day 45 were 0.89 ± 0.53% and 23.06 ± 7.32%, respectively. The frequencies of ssDNA-positive cells in the control group and irradiated group on day 9 were 0.13 ± 0.01 % and 0.31 ± 0.12 %, respectively. Finally, the frequencies of ssDNA-positive cells in the control group and irradiated group on day 45 were 0.18 ± 0.03% and 4.42 ± 2.95%, respectively.

3.2.2 *In vivo* NIR irradiation

NIR irradiation did not induce pain and the mice did not withdraw despite a lack of anesthesia during the NIR irradiation procedure. No side effects, such as epidermal burns, were observed during the study.

3.2.3 Histology of bone marrow

Hematopoietic bone marrow cell counts in the irradiated groups decreased significantly at day 7 and then increased gradually from day 30 to day 180 (Figures. 9-10). Significant decreases were observed between samples at days 7, 30, 90, and 180 as well as the non-irradiated controls at days 0 and 180 ($P < 0.05$).

The percentage of the area occupied by bone marrow adipocytes also increased dramatically at day 7, but gradually decreased thereafter. Significant increases were observed at days 7, 30, 90, and 180 compared to the non-irradiated controls at days 0 and 180 ($P < 0.05$).

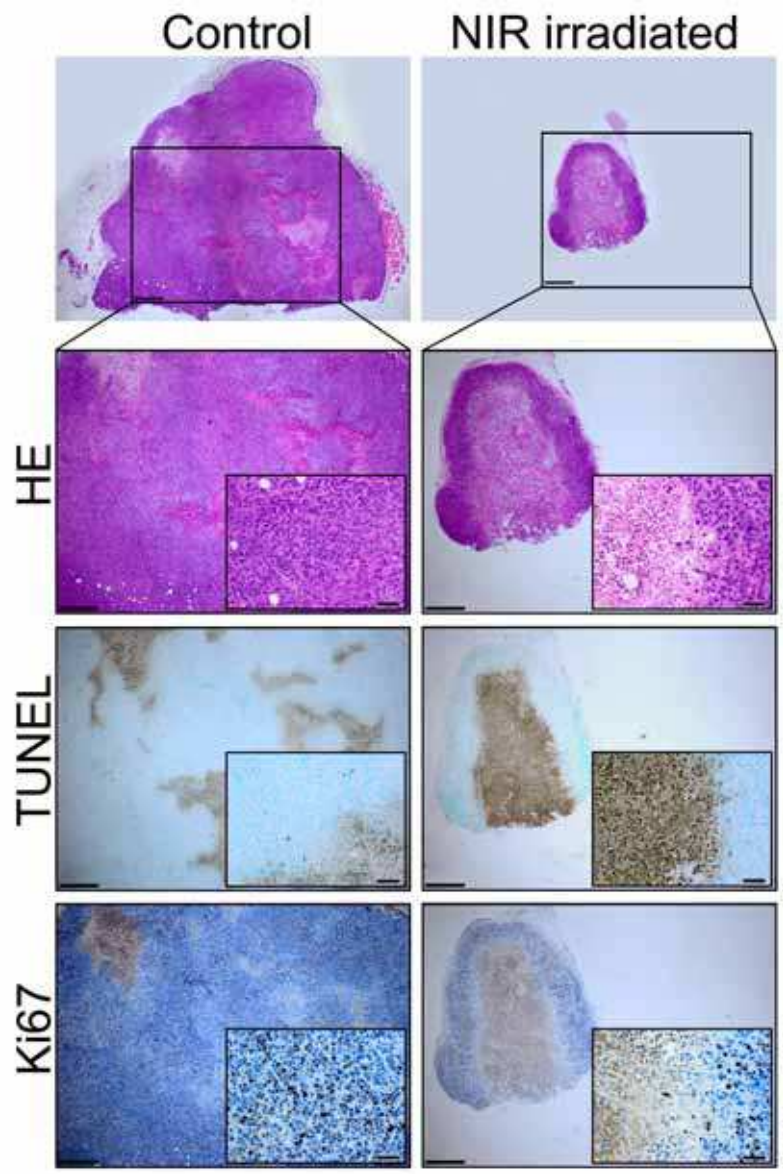

Fig. 4. Vertical histological sections of control and NIR irradiated MDA-MB435 melanoma tumors on day 45. The left column shows control tissues and the right column shows NIR irradiated tissues. Images from top to bottom show H&E staining, TUNEL staining, and immunohistological staining using an anti-Ki67 antibody. Scale bars = 400 μm (×40 magnification); insets: Scale bars = 40 μm (×400 magnification). Cited from Fig. 6(b). Tanaka et al. (2010). Non-thermal cytocidal effect of infrared irradiation on cultured cancer cells using specialized device. *Cancer Science.* 101:1396-402

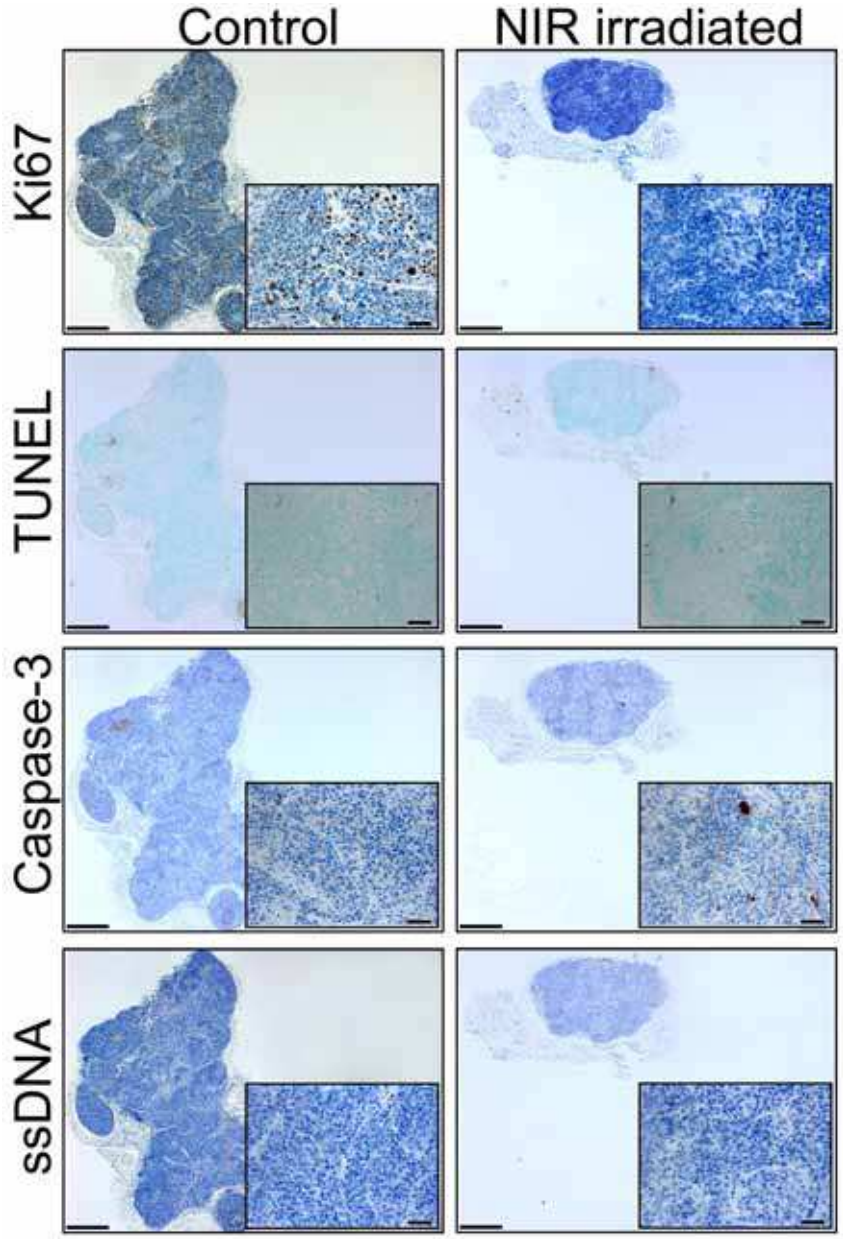

Fig. 5. Horizontal histological sections of control and NIR irradiated MDA-MB435 melanoma tumors on day 9. The left column shows control tissues and the right column shows NIR irradiated tissues. Images from top to bottom show immunohistological staining using an anti-Ki67 antibody, caspase-3, and single-stranded DNA. Scale bars = 400 μm (×40 magnification); insets: Scale bars = 40 μm (×400 magnification)

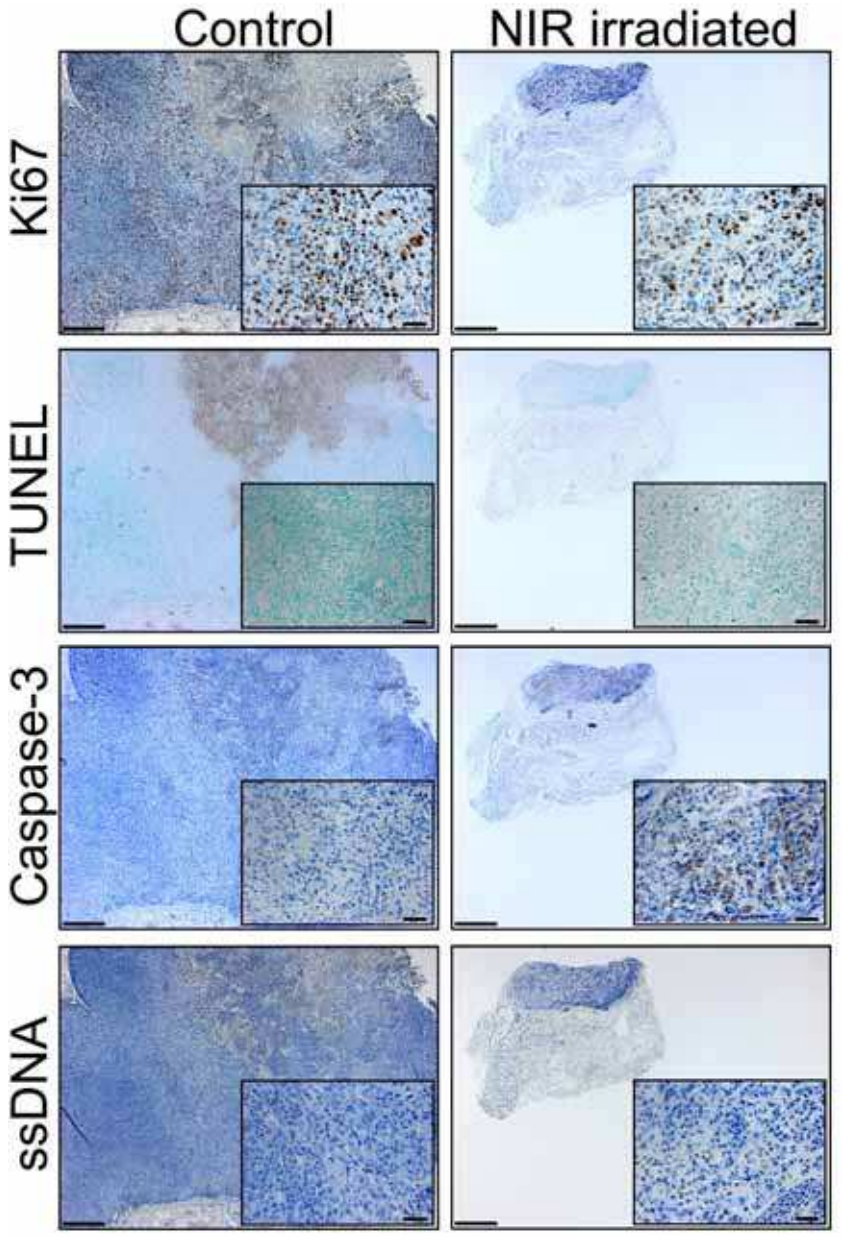

Fig. 6. Horizontal histological sections of control and NIR irradiated MDA-MB435 melanoma tumors on day 45. The left column shows control tissues and the right column shows NIR irradiated tissues. Images from top to bottom show immunohistological staining using an anti-Ki67 antibody, caspase-3, and single-stranded DNA. Scale bars = 400 μm (×40 magnification); insets: Scale bars = 40 μm (×400 magnification)

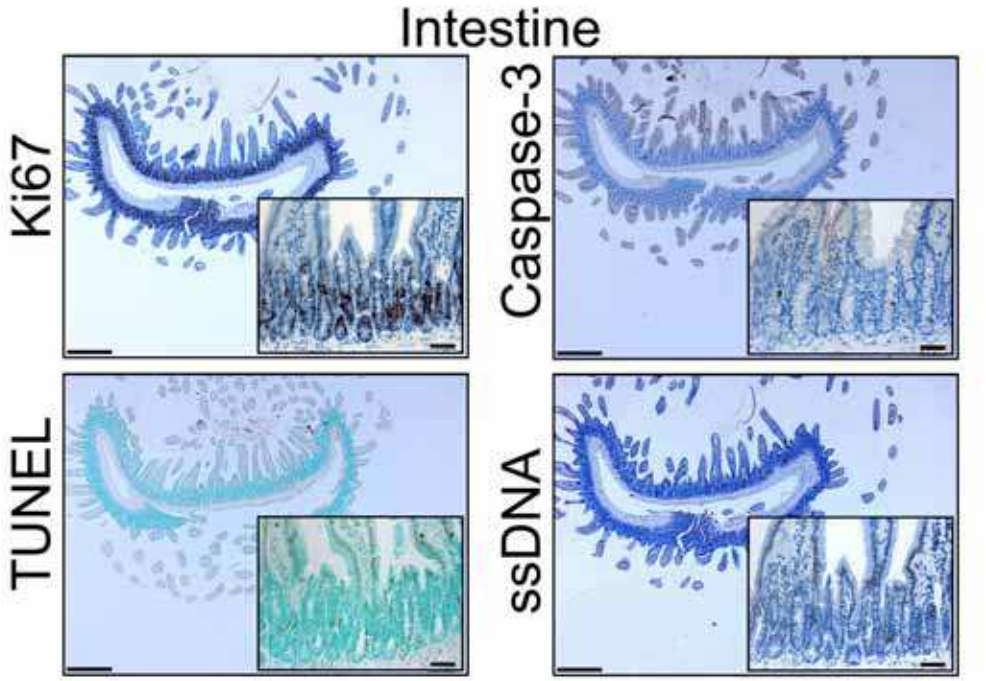

Fig. 7. Histological sections of intestine as a staining control. Images from top to bottom show immunohistological staining using an anti-Ki67 antibody, caspase-3, and single-stranded DNA. Scale bars = 400 μm; insets: Scale bars = 40 μm

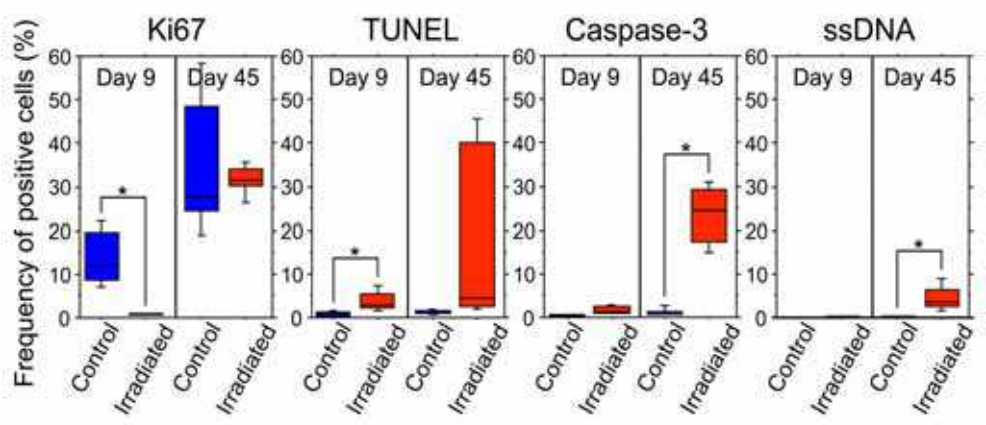

Fig. 8. Mean scores of frequencies of Ki67-, TUNEL-, caspase-3-, and ssDNA-positive cells. Significant differences (*: $P < .05$) between control and irradiated groups were observed in frequencies of Ki67-positive cells on day 9, TUNEL-positive cells, caspase-3-positive cells, and ssDNA-positive cells on day 45

The number of CD34-positive stem cells in the bone marrow dramatically increased at day 7, which persisted until day 180. Significant increases in cell number were observed on days 7, 30, 90, and 180 compared to the non-irradiated controls at days 0 and 180 ($P < 0.05$). Moreover, a majority of the CD34-positive stem cells in bone marrow were observed at the inner surface of the bone cortex.

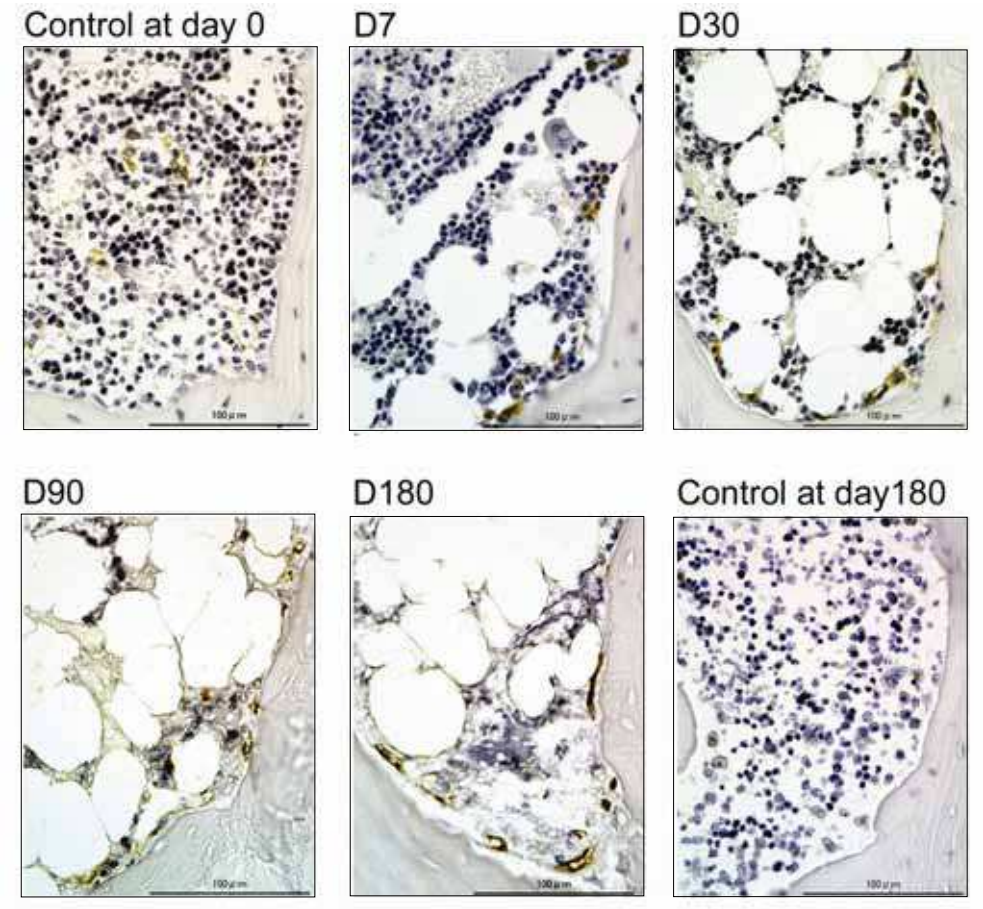

Fig. 9. Immunohistochemical staining of the spinous process with an anti-CD34 antibody

CD34-positive cells (stained brown) in the control at day 0 and 180 as well as the experimental samples at day 7, 30, 90, and 180 are shown. Scale bars = 100 μm.
Cited and revised from Fig. 2. Tanaka et al. (2011). Near-Infrared Irradiation Non-thermally affects Subcutaneous Adipocytes and Bone. *ePlasty.* 11:e12.
Hematopoietic bone marrow cell counts in the irradiated groups decreased significantly at day 7 and then increased gradually from day 30 to day 180. The percentage of the area occupied by bone marrow adipocytes also increased dramatically at day 7, but gradually decreased thereafter. The number of CD34-positive stem cells in the bone marrow dramatically increased at day 7, which persisted until day 180.

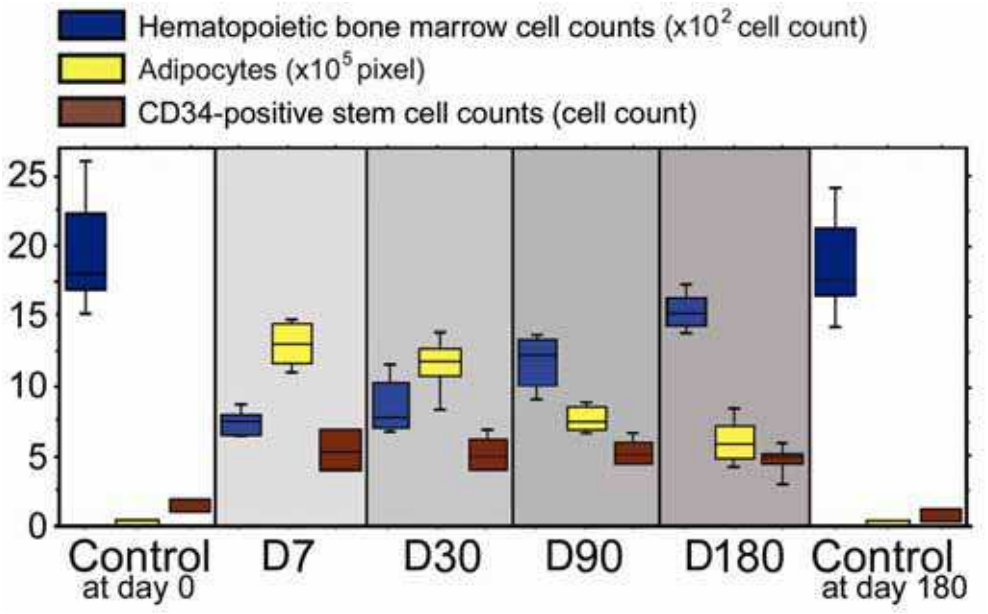

Fig. 10. Chronological changes in the hematopoietic bone marrow cell counts are indicated in blue, the percentage of the area occupied by bone marrow adipocytes in yellow, and the CD34-positive stem cell counts in brown

All were located in an area of superficial depth (1.5 mm) in the spinous process.
Cited and revised from Fig. 3 (b). Tanaka et al. (2011). Near-Infrared Irradiation Non-thermally affects Subcutaneous Adipocytes and Bone. *ePlasty*. 11:e12.

4. Discussion

4.1 UV and NIR in the natural sunlight

Individuals enjoy spending time under the sun, and UV blockers are often used to prevent skin damage by UV exposure. Exposure to UV radiation is the most important environmental carcinogen (Travers et al., 2008) and plays a significant role in the development of melanoma (Wolf et al., 1994).
Sunscreens reduce the effects of UV radiation on human skin (Ananthaswamy et al., 1997). Nevertheless, sunscreens have failed to protect against the increase in UV radiation-induced melanomas (Wolf et al.,1994). Various kinds of UV blocking materials, such as sunblocks, films, paints, and fibers are often used to prevent skin damage from UV exposure. Although individuals all over the world use various types of sunscreens, unwanted biological influences, such as rosasea, erythema ab igne, long-term vasodilation (Tanaka et al., 2011c), muscle thinning, and sagging still occur (Tanaka et al., 2010c). Most sunscreens can only block UV, but not visible light and IR (Tanaka & Matsuo, 2008).
In natural sunlight, however, humans are also continually exposed to IR. Solar IR that reaches the Earth's surface is predominantly infrared. In actuality, 54.3% of incident solar energy is composed of infrared, whereas the energy contributions of UV and visible light

radiation are 6.8 and 38.9%, respectively (Kochevar, 1999). IR radiation ranging from 760 nm to 1 mm is non-ionizing radiation located 'below the red', i.e. adjacent to the red part of the visible radiation range and extending up to the microwave range. The IR spectral region is arbitrarily divided according to wavelength into sub-regions of NIR (760–3000 nm), middle IR (3000–30 000nm), and far IR (30 000 nm–1 mm). NIR radiation from the sun is selectively filtered by atmospheric water (Anderson & Parrish, 1981; Gates, 1966); thus, most NIR radiation that reaches the Earth's surface readily penetrates the superficial layers of the skin. In addition to natural NIR, human skin is increasingly exposed to artificial NIR from medical devices and electrical appliances (Schieke et al., 2003; Schroeder et al., 2008). Therefore, we are exposed to tremendous amounts of NIR every day (Tanaka & Matsuo, 2008).

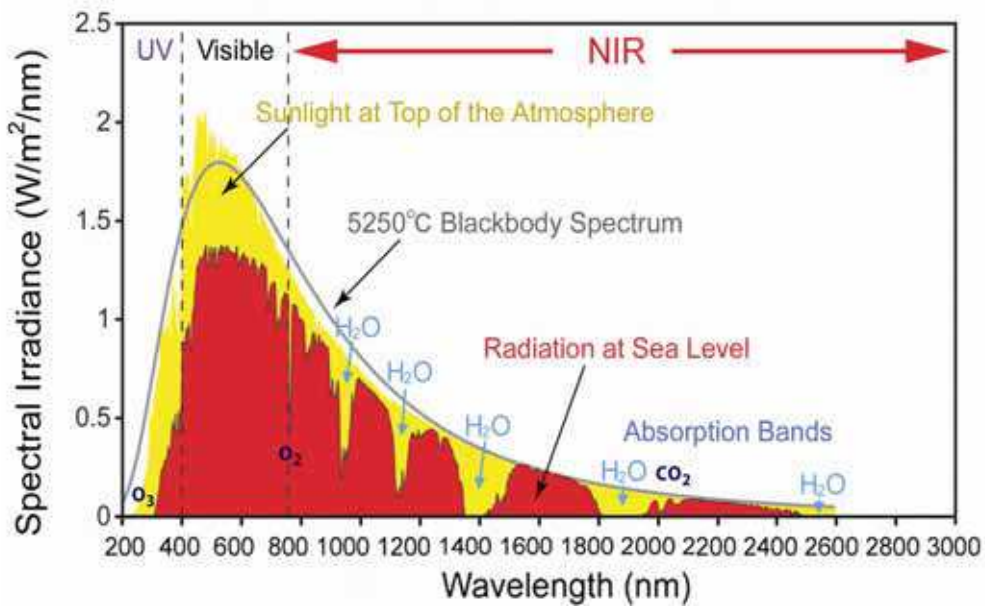

Fig. 11. Solar radiation. This graph shows the radiation spectrum for direct light both at the top of the Earth's atmosphere (yellow) and at sea level (red). The sun produces light with a distribution similar to that expected from a 5250°C blackbody (gray), which is approximately the temperature of the Sun's surface. As light passes through the atmosphere, some is absorbed by gases with specific absorption bands (blue). These curves are based on the American Society for Testing and Materials Terrestrial Reference Spectra, which are standards adopted by the photovoltaic industry to ensure consistent test conditions and are similar to the light levels expected in North America. Regions for UV, visible, and NIR are indicated

Cited and revised from Fig. 2. Tanaka et al. (2010). Long-lasting muscle thinning induced by infrared irradiation specialized with wavelength and contact cooling: A preliminary report. *ePlasty.* 10:e40.
Mr. Robert Rohde (GlobalWarmingArt.com) generously gave us precise data and the file for this figure.

4.2 Properties of NIR

NIR is an electromagnetic wave that simultaneously exhibits both wave and particle properties and is strongly absorbed by water, hemoglobin, and myoglobin (Tanaka et al., 2011c). As a consequence, NIR irradiation can penetrate the skin and affect the subcutaneous tissues, including muscles and bone marrow, with both its wave as well as its particle properties.

NIR irradiation was shown to induce the expression of collagen (Tanaka et al., 2009a), elastin, and water-binding proteins (Tanaka et al., 2009a, 2009b) without scar formation (Tanaka et al., 2010a). Further, near-infrared irradiation non-thermally induced long-lasting muscle thinning (Tanaka et al., 2010c), muscle relaxation (Tanaka et al., 2011a), bone marrow damage (Tanaka et al., 2011b), a cytocidal effect on cancer cells (Tanaka et al., 2010b), and stimulation of stem cells (Tanaka et al., 2011b).

The penetrating 600-1300 nm wavelength region causes photochemical changes and affects a large volume and depth of tissue (Anderson & Parrish, 1981). Actively proliferating cells show increased sensitivity to red and NIR (Karu et al.,1994; Tafur & Mills, 2008). NIR irradiation induces strand breaks and apoptosis (Tirlapur & König, 2001) as well as cell death of cancer cells and bone marrow cells (Tanaka et al., 2010b, 2011b). NIR irradiation is used as a therapeutic option in the treatment of wound healing disorders (Danno et al., 2001; Horwitz et al., 1999; Schramm et al., 2003) and malignant tumors (Bäumler et al., 1999; Dees et al., 2002; Kelleher et al., 1999; Orenstein et al., 1999). While NIR irradiation appears to damage tumor tissue, it has also been shown to reduce cellular protein damage produced by biological oxidants in normal cells (Kujawa et al., 2004).

4.3 The effects of NIR on human skin

Both UV and visible light radiation are attenuated by melanin (Anderson & Parrish, 1981), whereas NIR is strongly absorbed by hemoglobin and fluids. We previously reported that NIR is absorbed by sweat on the skin surface, water in the dermis, and hemoglobin in dilated vessels (Tanaka et al., 2009b, 2011c). The dermis tends to increase the amount of fluid by inducing an increase in collagen, elastin, and water-binding protein in order to protect subcutaneous tissues from NIR (Tanaka et al. 2009a, 2009b). Pre-exposure of NIR prevents UV-induced toxicity (Danno K et al., 1992; Frank et al., 2004; Menezes et al., 1998), and this effect is independent of heat shock protein induction and cell division (Menezes et al., 1998). These findings suggest that NIR irradiation prepares skin to better resist the subsequent damage of UV or NIR.

Similar to UV, NIR seems to exert biologic effects on human skin (Schieke et al., 2003). NIR irradiation was shown to cause skin changes similar to those observed in solar elastosis, and enhanced UV-induced dermal damage (Kligman, 1982). NIR irradiation is able to activate mitogen-activated protein kinases and induce gene transcription and is likely to increase collagen degradation (Kim et al., 2006; Schieke et al., 2003; Schroeder et al., 2008). NIR radiation elicits a retrograde signaling response, which subsequently induces an increase in dermal MMP-1 expression that is a key symptom of photoaging. Epidemiological data and clinical reports points to the ability of NIR to cause and enhance actinic skin damage, implying that NIR is not innocuous to human skin (Kligman LH & Kligman AM, 1984; Dover et al., 1989; Schieke et al., 2003).

Both thermal and non-thermal damage to tissue can occur when skin is exposed to NIR radiation.

The mean facial surface area that is covered with wrinkles is significantly smaller in African Americans than in Caucasians, and characteristics of age-related periorbital changes seem to occur at a more accelerated rate in Caucasians (Odunze et al., 2008). In addition, fair skin is more sensitive to skin aging (Guinot et al., 2002; Nagashima et al., 1999). These findings support the observation that fair skin tends to wrinkle and sag earlier in life (Rawlings, 2006; Tsukahara et al., 2004), because fair skin is thinner and is more susceptible to NIR damage to the underlying frontalis, orbicularis oculi, and platysma muscles than dark skin (Tanaka & Matsuo, 2008). NIR is attenuated by thick water-containing dermis. Thus, skin with sparse melanin and a thin dermis might allow NIR radiation to penetrate deeper into human tissue than skin with dense melanin and a thick dermis.

Repeated exposure to sources of heat and NIR, such as fires and stoves, results in a skin lesion described as erythema ab igne (Findlayson et al., 1996), which is clinically characterized by a reticular hyperpigmentation and teleangiectasia accompanied histologically by epidermal atrophy, vasodilation, and dermal melanin and hemosiderin deposits. After many years, these lesions may develop thermal keratoses, such as hyperkeratosis, keratinocyte dysplasia, and dermal elastosis which are similar to the changes that occur in actinically damaged skin (Arrington & Lockman, 1979). Similar to actinic keratoses, thermal keratoses are precancerous lesions that exhibit epidermal dysplasia, which may develop into invasive squamous cell carcinoma. There are several reports of carcinomas arising from heat induced erythema ab igne (Kligman LH & Kligman AM, 1984; Hewitt et al., 1993; Jones et al., 1988). NIR radiation, similar to UV radiation, induces photoaging and potentially photocarcinogenesis (Schieke et al., 2003). In addition, skin tumors in mice appeared faster after irradiation with the full lamp spectrum containing UV, visible, and NIR compared to irradiation with UV alone (Bain et al., 1943).

4.4 The effect of NIR on human subcutaneous tissues

Although there have been many studies regarding the superficial effects of NIR irradiation, the damage of deeper tissues has not been well investigated. Since the permeability of NIR is extremely high, the influence on deeper tissues should be considered.

NIR is an electromagnetic wave that simultaneously exhibits both wave and particle properties and is strongly absorbed by water, hemoglobin, and myoglobin (Tanaka et al., 2011c). As a consequence, NIR irradiation can penetrate the skin and affect the subcutaneous tissues (Tanaka et al., 2009a, 2009b), including muscle and bone marrow (Tanaka et al., 2010c, 2011a, 2011b).

NIR radiation induces vasodilation, collagen, and elastin, and increases the number of superficial granular adipocytes to protect the deeper tissues against NIR (Tanaka et al., 2011b). Continual long-term exposure to incident solar NIR radiation causes long-lasting thinning of the superficial facial muscles and the muscle extensions to the dermis, which ultimately leads to facial skin ptosis. Additional factors that are thought to contribute to brow ptosis include the gradual loss of forehead skin elasticity and a reduction in the tone of the frontalis muscles (Knize, 1996; Niechajev, 2004). The use of NIR irradiation for smoothing forehead wrinkles also caused brow ptosis. These results may have major implications in superficial tissue aging.

The widespread use of sunscreens has helped to reduce some of the deleterious effects of UV radiation on human skin (Ananthaswamy et al., 1997), however sunscreens that protect

from NIR radiation should also be used to prevent damage to deeper tissues (Tanaka & Matsuo, 2008; Tanaka et al., 2010c, 2011b, 2011c).

4.5 NIR device

NIR irradiation is known to induce dermal heating, which results in skin laxity tightening. Many studies have shown the influence of superficial tissues. For example, wavelength selection directly influences target selection and penetration depth (Figure 1.).

NIR devices without a water filter or contact cooling have been used in previous studies to evaluate photobiological effects on the human body. However, with these treatments, a substantial amount of energy is absorbed in the superficial layers of skin and only limited NIR energy can be delivered to deeper tissues. Wavelengths below 1100 nm are preferentially absorbed by melanin in the superficial layers of the skin. Wavelengths between 1400 and 1500 nm and those above 1850 nm are absorbed heavily by water in the superficial layers of the skin, which results in heating and can lead to painful sensations and burns (Kelleher et al., 1999). NIR radiation from the sun is selectively filtered by atmospheric water (Anderson & Parrish, 1981; Gates, 1966); thus, most NIR radiation that reaches the Earth's surface readily penetrates the superficial layers of the skin.

In this study, we used an NIR device that emitted a spectrum of NIR irradiation from 1100 to 1800 nm with a water-filter that excluded wavelengths between 1400 and 1500 nm, which are strongly absorbed by water and hemoglobin (Figure. 1). Filtering out the wavelengths below 1100 nm, around 1450 nm, and above 1850 nm enabled for the delivery of NIR irradiation to deeper tissues (Davenport et al., 2006) and also simulated solar NIR radiation that reaches the skin of humans on the Earth's surface. Therefore, an NIR device with a water-filter mimics the natural situation and allows for the evaluation of solar NIR radiation that reaches the skin. However, in reality, both solar NIR radiation with an atmospheric water filter and the NIR device with a water filter increase the skin surface temperature and induce perspiration and blood vessel dilation that mediate the absorption of NIR radiation by water and hemoglobin, respectively. To counter this effect, in this study, we used contact cooling through a temperature-controlled sapphire window to reduce the skin surface temperature and thereby reduce perspiration and blood vessel dilation.

These specific wavelengths and the cooling system enabled NIR irradiation to penetrate the skin surface without pain or epidermal burns (Davenport et al., 2006; Goldberg, et al., 2007), which was evidenced by the ability to treat animals and humans without anesthesia and without contact burns or other adverse events.

4.6 The effects of NIR on cancer cells

4.6.1 Wavelength of NIR anticancer therapy

Photodynamic therapy (PDT) is the most common antitumor therapy using IR for select forms of cancer (Dougherty et al., 1998). Photodynamic therapy is based on the accumulation of a photosensitizing agent in tumors and uses wavelengths near 800 nm as a photoactivating wavelength to achieve maximum penetration depth (Bäumler et al., 1999; Lobel et al., 2001; Orenstein et al., 1999). This wavelength, however, also has high melanin absorption, which limits the ability to deliver light to highly pigmented tumors (Busetti et al., 1998).

Although wavelengths near 800 nm are the standard activators for PDT, other wavelengths have also shown treatment promise. Santana et al. reported that NIR at 904 nm may have

antitumor activity, as shown by an increase in cytomorphological changes as well as apoptosis in neoplastic cells (Santana-Blank et al., 2002). In a study using NIR irradiation at 904 nm, irradiation was shown to increase cytomorphologic changes with programmed cellular death in neoplastic cells; however, no apparent changes were observed in non-neoplastic cells (Santana-Blank et al., 2002). Unlike wavelengths beyond 1100 nm, where melanin absorption is negligible (Anderson & Parrish, 1981), absorption at 904 nm was significant. This may limit the possible uses of the 904 nm wavelength for certain body areas in races with skin that is rich in melanin.

Actively proliferating cells show increased sensitivity to red and IR irradiation (Karu et al., 1994; Tafur & Mills, 2008). IR irradiation alone appears to induce DNA strand breaks and apoptosis (Tirlapur & König, 2001), which elicits photodisruptive destruction of tumor tissue (Dees et al., 2002). While IR irradiation appears to damage tumor tissue, it has also been shown to reduce cellular protein damage produced by biological oxidants in normal cells (Kujawa et al., 2004).

Various types of IR devices and lasers are used in antitumor therapies, such as PDT and hyperthermia, and typically utilize wavelengths between 750 to 3000 nm. Wavelength selection directly influences target selection and penetration depth, and wavelengths below 1100 nm are absorbed preferentially by melanin in the superficial layers of skin (Figure. 1). Wavelengths between 1400 to 1500 nm and above 1850 nm are absorbed heavily by water, which results in the heating of the superficial layers of the skin. The delivery of NIR energy safely to deeper tissues without significant superficial heating requires wavelengths between 1100 nm and 1850 nm, excluding the range from 1400–1500 nm (Davenport et al., 2006).

Although many studies have shown the thermal effects of NIR irradiation on cancer cells in the field of hyperthermia, non-thermal effects of NIR irradiation were not investigated in detail. We first reported on the non-thermal effects of NIR irradiation using a specialized broad spectrum light source emitting light between 1100–1800 nm (with a filter to exclude wavelengths between 1400 and 1500 nm) on cancer cells and suggested the possibility of beneficial uses for cancer treatment (Tanaka et al., 2010b).

4.6.2 The effects of NIR on *in vitro* cancer studies

In our *in vitro* studies, proliferation of MDA-MB435 and B16F0 melanoma cells was significantly suppressed by NIR irradiation. Total NIR output appeared to correlate with cell survival. NIR irradiated cell cultures showed significant decreases in cell counts in all cultures, except at the lowest dose of irradiation in group 20 J x 3. A correlation with efficacy seemed to be highest with total delivered energy, and not per pulse fluence, since multiple irradiations with a lower output appeared equally effective as higher fluence irradiations. Ten exposures at 20 J/cm^2 achieved a comparable significant reduction in cell count as that of 3 exposures at 40 J/cm^2. In addition, three exposures at 20 J/cm^2 appeared close to a threshold energy dosage. Further studies are required to determine the accurate correlations between irradiation dose and cell survival as well as the different effects on each cancer cell line.

In our previous studies, increased temperature appeared not to play a role in the cell culture survival rate. Results in the 20 J/cm^2 group (excluding group 20 J x 3) were statistically equivalent to the 40 J/cm^2 group, and the maximum temperature rise during exposure in the 20 J/cm^2 group was only 3.76˚C (temperature = 40.76˚C). This is roughly equivalent to a illness-induced fever. In addition, elevated temperatures only remained above 40˚C for 3.6

seconds, which was far short of the damages observed during prolonged high-grade fevers. The rationale of hyperthermia is based on a direct cytocidal effect at temperatures above 41-42°C (Dewey, 1994). With whole-body hyperthermia, tumor growth suppression requires temperatures of approximately 42°C and an exposure of at least 60 minutes (Wust et al., 2002). Although the extent and duration of temperature elevation were not significant in relation to the cases of hyperthermia, irradiated cell cultures showed significant decreases in cell counts in our studies. This level of temperature rise was not associated with tumor growth suppression, indicating a factor other than hyperthermia is responsible for growth suppression of these cancer cell lines. NIR is known to induce molecular vibrations (Pujol & Lecha, 1993; Schieke et al., 2003). The molecular vibrations of water and the resonance of alpha helices in proteins appeared to be related to the cytocidal effect of NIR on cancer cells.

4.6.3 The effects of NIR on *in vivo* cancer studies

In our *in vivo* studies, NIR irradiation significantly inhibited the tumor growth of MDA-MB435 melanoma cells transplanted in nude mice *in vivo*. Significant differences between the control and irradiated groups were observed for tumor volume and frequencies of Ki67-positive, TUNEL-positive (Tanaka et al., 2010b), activated caspase-3, and single-stranded DNA-positive cells.

The histological findings showed tumor shrinkage and dying cells in the center of the tumor mass, which supports the hypothesis that NIR electromagnetic properties induce these biological effects non-thermally.

NIR penetrates the skin and reaches the subcutaneous tissues without a significant increase in skin temperature (Schieke et al., 2003). The effects of NIR are independent of the generation of heat (Danno et al., 2001). If the cytocidal effect of NIR was induced thermally, the histology would show a gradient cytocidal effect from the superficial layer to the center of the tumor, and thermal effect would be reduced by the contact cooling (20 °C) of the NIR device. Due to surface cooling, NIR can penetrate deeper tissue and induce a drastic non-thermal cytocidal effect in the center of the tumor mass.

NIR treatment with very low output and fewer exposures (10 exposures of NIR at 20 and 40 J/cm^2) also inhibited tumor growth. This output was so low that on human skin, the sensation of heat would not be felt due to contact cooling. This NIR irradiation induced no pain, and the mice did not withdraw from the treatment even though NIR treatment was performed without anesthesia. In addition, side effects, such as epidermal burns, were not observed, and the mice looked healthy throughout the study. Further studies are necessary to determine if more output, increased frequency of treatments, and/or longer periods of irradiation may be even more effective in suppressing tumor growth.

It is still unknown why NIR induces a cytocidal effect in cancer cells. However, we found that NIR induced muscle thinning (Tanaka et al., 2010c, 2011a), bone marrow damage (Tanaka et al., 2011b), and a cytocidal effect in cancer cells (Tanaka et al., 2010b), which was most likely due to a different type of apoptosis. A significant reduction in tumor volume and a high level of TUNEL-positive cells in the irradiated group indicated that NIR irradiation induces apoptosis in cancer cells. The frequency of Ki67-positive cells on day 9 in the irradiated group were significantly lower than the control group, which supports the hypothesis that NIR irradiation can suppress the proliferation of cancer cells. However, the mechanism of NIR-mediated tumor cell death appeared to be different than standard apoptosis because high levels of activated caspase-3 expression and ssDNA-positive cells appeared gradually after NIR irradiation, although tumor shrinkage happened rapidly.

On the other hand, NIR irradiation induced the stimulation of CD34-positive bone marrow stem cells in our previous study (Tanaka et al., 2011b), and the frequency of Ki67-positive cells on day 45 was significantly higher than the irradiated group on day 9. These results suggest that NIR irradiation may stimulate stem cells.
The immunohistological staining results suggested that NIR may induce cell death of highly proliferative tumor cells, stimulate stem cells, and then induce apoptosis of the cells which are unnecessary to promote the development of melanoma. These steps appeared to be a part of the mechanism driving the effects of NIR on cancer cells.
The advantages of this NIR irradiation schedule include reducing discomfort, limiting side effects, and the low cost. Taken together, these characteristics were facilitated by repeated irradiations, which if proven beneficial for cancer cell reduction in humans, may provide an alternative or adjunct treatment for a transient mass reduction before surgery, offer improved results, and/ or improve patient quality-of-life. NIR irradiation is frequently administered at a level of 40 J/cm^2 for other indications, with a very high safety record and no significant complications (Goldberg et al, 2007).

4.6.4 The effect of NIR on molecular structure: is it mainly alpha helices?

NIR is absorbed by water, hemoglobin, and myoglobin. The NIR spectrum of biological materials is a result of the overtones and combination of O-H, C-H, and N-H groups' bond stretching vibrations (Weyer, 1985). Water is a polar molecule with an electrical dipole moment and possesses hydrogen bonds. A water molecule will be resonated by NIR and absorb NIR due to the O-H intramolecular hydrogen bonds and electrical dipole moment (Tsai et al., 2001). Since T2 weighted MRI enhances water as well as active proliferating cancer cells, active proliferating cells may have a rich water content, which strongly absorbs NIR.
Hemoglobin has four heme-binding subunits, each largely made of alpha helices, and myoglobin consists of eight alpha helices that are connected through turns with an oxygen binding site. The similarity between hemoglobin and myoglobin resides in the heme binding sites and alpha helices. Heme is a prosthetic group that consists of an iron atom located in the center of a large heterocyclic organic ring called porphyrin. Our results of long-lasting muscle thinning and vasodilation induced by NIR suggest that NIR might resonate and damage heme. However, our collagen, elastin, and cancer studies suggest that NIR may mainly resonate helical structures, alpha helices, and DNA. Alpha helices are thought to be resonated by NIR and have strong amide bands in the IR spectra, which have characteristic frequencies and intensities (Nevskaya & Chirgadze, 1976). Both hemoglobin and myoglobin are the oxygen-carrying proteins and have many alpha helices. It is possible that NIR induces resonance of alpha helices in the oxygen-carrying proteins and degenerates proteins containing alpha helices, which results in damage to the storage and transport of oxygen. This could be one of the mechanisms of apoptosis. In our previous study, we evaluated the effect of NIR on myoglobin; however, similar effects may also be found for hemoglobin (Tanaka et al., 2011c).
NIR increases the amount of water retained in the dermis by inducing vasodilation and the expression of collagen and elastin (Tanaka et al., 2009b). Both collagen and elastin possess helical structures and hydrogen bonds. Elastin has higher absorption properties than that of water (Tsai et al., 2001). These findings suggest that we have acquired biological defense mechanisms in which induced helical structures and hydrogen bonds are resonated by NIR and absorb NIR to protect the subcutaneous tissues against NIR.

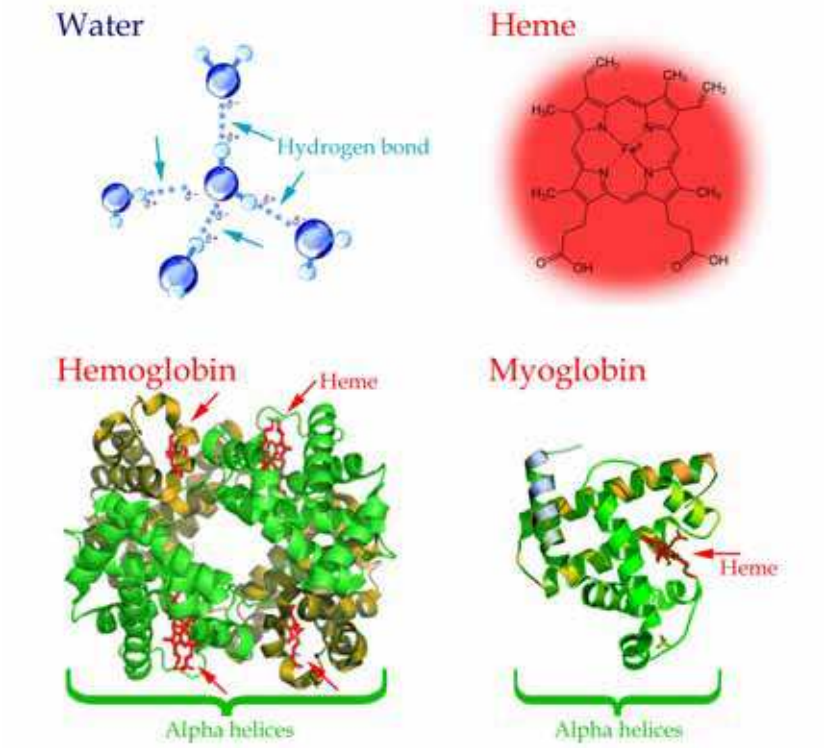

Fig. 12. The structure of water, heme, hemoglobin, and myoglobin. Water is a polar molecule with an electrical dipole moment and possesses hydrogen bonds (*light blue dots*). Heme is a prosthetic group that consists of an iron atom located in the center of a large heterocyclic organic ring called porphyrin. The hemoglobin molecule has four heme-binding subunits, each largely made of alpha helices (*green*). Myoglobin consists of eight alpha helicies (*green*) and possesses heme as an oxygen binding site. The red arrow indicates heme. Cited and revised from Wikipedia

Similarly, DNA consists of two long strands in the shape of a double helix, which is stabilized by two forces: hydrogen bonds between nucleotides, and base-stacking interactions among the aromatic bases. Many studies regarding DNA and cancer imaging have been performed using an NIR spectroscopy, since biological molecules such as proteins, lipids, and nucleic acids provide a unique absorption spectral pattern, and NIR induces the vibration of DNA. IR irradiation alone appears to induce DNA strand breaks and apoptosis (Tirlapur & König, 2001). DNA will be also resonated and absorb NIR, which is most likely due to its helical structures.

4.6.5 The effects of NIR on lamin

The nuclear lamina is a proteinaceous structure located underneath the inner nuclear membrane that forms a stress-resistant elastic network where it associates with the peripheral chromatin (Prokocimer et al., 2009). It contains lamins and lamin-associated proteins, including many integral proteins of the inner nuclear membrane, chromatin

modifying proteins, transcriptional repressors, and structural proteins (Hutchison & Worman, 2004; Mounkes & Stewart, 2004; Smith et al., 2005; Broers et al., 2006).

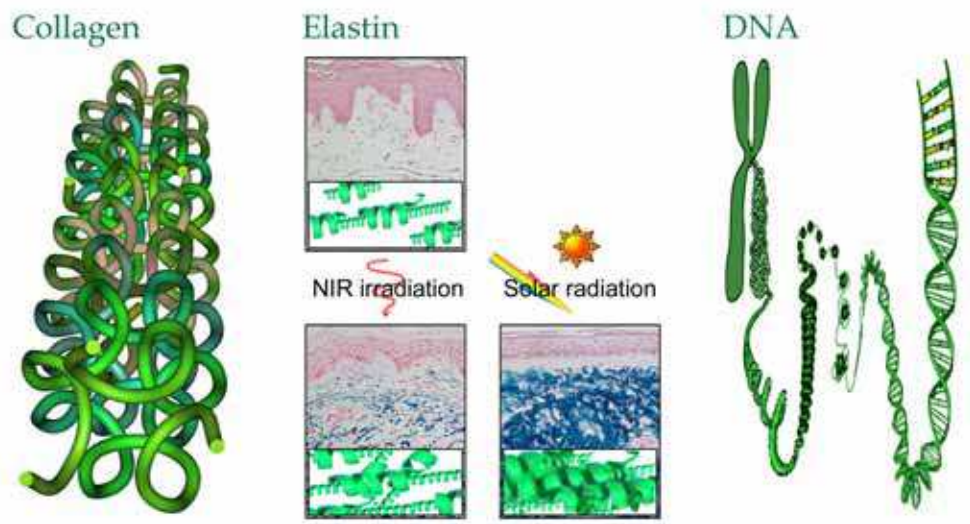

Fig. 13. The structure of collagen, elastin, and DNA. Collagen (left), elastin (center), and DNA (right) possess many alpha helices. Representative histologies of sun-protected skin (center, left) and sun-exposed skin (center, right) stained with Victoria Blue stain. Sun-protected skin taken from the thigh of a 33-year-old Japanese man. Control skin (center, above). Thirty days after NIR irradiation at 36 J/cm² (center, below). Sun-exposed skin taken from the cheek of a 72-year-old Japanese female (center, right). Solar elastosis stained blue are observed in the dermis.A schema of elastic fibers (green) is enclosed in the smaller box below each picture. Cited and revised from Wikipedia for collagen and DNA structures

Lamins are type-V intermediate filament proteins located in the nucleus, primarily in the periphery, and underlie the nuclear envelope (Mounkes & Stewart, 2004). Lamins have a conserved alpha helical central rod domain and variable head and tail domains (Prokocimer et al., 2009; Stuurman et al., 1998; Zaremba-Czogalla et al., 2011) (Fig. 14). Alpha helical structures are surmised to absorb NIR and protect the nucleus and DNA from NIR. The nuclear lamina was thought to provide structural support to the nucleus and protect the peripheral chromatin; however, it is now known that the nuclear lamina is involved in a number of fundamental molecular processes ranging from DNA replication and RNA transcription (Spann et al., 2002) to genome silencing and DNA repair (Reddy et al., 2008). The lamins and their associated proteins are required for most nuclear activities, including mitosis, and for linking the nucleoplasm to all major cytoskeletal networks in the cytoplasm. The lamin A gene has been linked to longevity and was proposed to be a guardian of somatic cells during their lifetime (Hutchison & Worman, 2004). Mutations in the lamin A gene cause a spectrum of 20 age-related human disorders, termed laminopathies, which affect the maintenance of one or more tissues of mesenchymal origin. Remarkably, many tissues affected by mutations in the lamin A gene are also affected in many degenerative conditions common to old age. The compromised tissue functions in laminopathy diseases

are proposed to be a consequence of decreased cellular proliferation (Pekovic et al., 2007), a failure to maintain a differentiated state, and/or a loss of tissue repair during regeneration (Mounkes & Stewart, 2004; Bakay et al., 2006). Lamin A knock-out mouse models as well as mutated lamin A knock-in or transgenic mice manifesting either muscular dystrophy (Sullivan et al., 1999; Arimura et al., 2005) or premature ageing (Mounkes et al., 2003; Yang et al., 2005; Varga et al., 2006) have shortened lifespans and die prematurely. Moreover, mouse models null for the pre-lamin A gene also have shortened lifespans and show progeria-like pathologies of bone and muscle (Bergo et al., 2002; Pendas et al., 2002).

Lamins play important roles in DNA replication, chromatin organization, adult stem cell differentiation, aging, and tumorigenesis. In addition, mutations in lamin lead to laminopathic diseases (Prokocimer et al., 2009).

Nuclei assembled in vitro in the absence of lamins are more prone to breakage than nuclei assembled in the presence of a full complement of lamins (Sullivan et al., 1999; Newport et al., 1990). Disruption of the lamins results in abnormal mitosis, chromosomal segregation, and cell death (Liu et al., 2003).

During mitosis, lamin molecules are transiently disassembled into monomers (Gerace & Blobel, 1980; Yang et al., 1997) through phosphorylation (Peter et al., 1990) by the protein kinase p34cdc2 (Nigg, 1992). In addition, actively proliferating cells show increased sensitivity to NIR (Karu et al., 1994; Tafur & Milles, 2008), and IR irradiation induces DNA strand breaks and apoptosis (Tirlapur & König, 2001). Therefore, these findings suggest that NIR exposure appears to damage nuclear lamins and DNA in the mitotic phase due to absence of nuclear lamins protection, which results in apoptotic cell death.

Thus, NIR irradiation has a potential application for transient mass reduction of proliferative malignant cancer, such as breast cancer and melanoma before surgery (Tanaka et al., 2010b), or for the treatment for terminal patients.

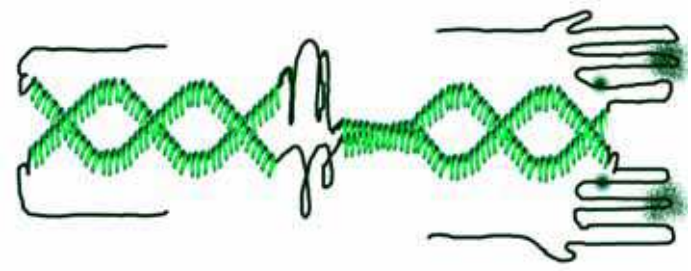

Fig. 14. The structure of lamin dimers. A pair of alpha helical central rods forms the lamin dimer. Cited and revised from Prokocimer, et al (2009). Fig. 1. Nuclear lamins: key regulators of nuclear structure and activities. *J Cell Mol Med.* 13(6):1059-85

4.6.6 Lamin and cancer

Malignant transformation is a multi-step process of sequential alterations that occur in the critical genes involved in cancer regulating pathways as well as various mediators, which mediate the "cross-talk" between them. These molecular events are accompanied by nuclear structural alterations, which are involved in common diseases, particularly cancer (Foster et al., 2010), and differentiate cancer cells from normal cells (Prokocimer et al., 2009). Nuclear lamins are responsible for the distortion of the nuclear envelope, and nuclear margin

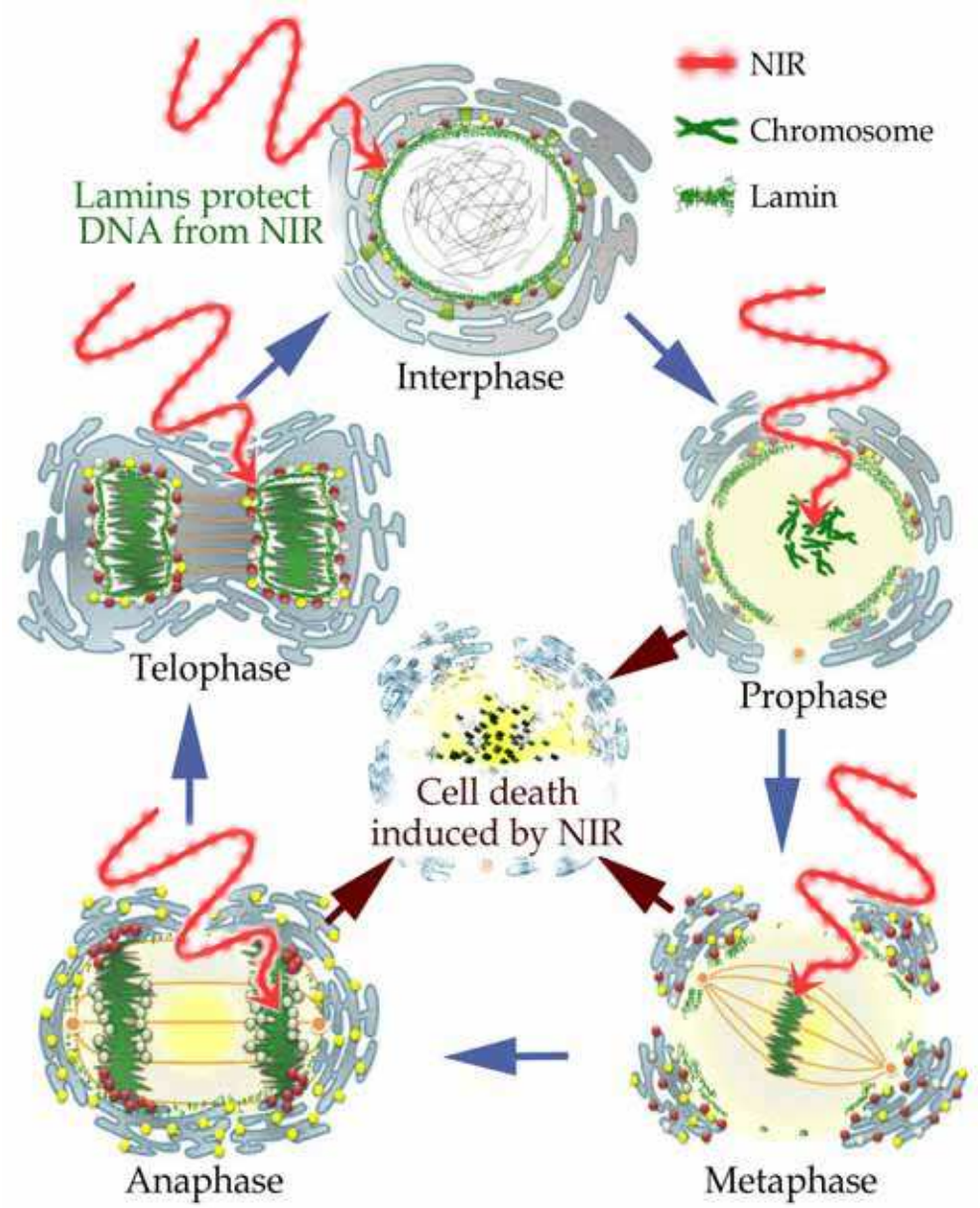

Fig. 15. A schematic of the cell cycle and effects of NIR. NIR cannot penetrate the nuclear envelope due to the protection of nuclear lamins in interphase and telophase. NIR may damage the chromosomes of mitotic cells in prophase, metaphase, and anaphase due to the absence of nuclear lamin protection, which results in apoptotic cell death. Cited and revised from Wikipedia

irregularity is an important diagnostic feature of malignant cells (Dey, 2009). Lamin expression in tumor cells may potentially serve as a cancer-related biomarker for diagnosis, prognosis, and surveillance. Alterations of the nuclear lamina are being recognized as an additional event involved in malignant transformation (Prokocimer et al., 2009). Altered lamin expression in cancer cells contributes to the characteristic changes in nuclear architecture, including alterations of nuclear structure and chromatin texture, which occurs in all cancer subtypes (Zink D et al., 2004).

Nuclear lamins also have a crucial role in maintaining chromosomal stability for the prevention of cancer progression, and are also involved in tumor suppressive pathways that trigger apoptosis or senescence (Prokocimer et al., 2009). Thus, alterations in lamins allow cancer cells to escape the normal control of cell proliferation and cell death, which yields a pro-cancerous effect (Vogelstein & Kinzler, 2004). Lamin A is absent in hyperproliferative basal cell skin carcinomas, and its presence or absence may directly influence the proliferative status of the tumor (Venables et al., 2001). Moreover, the poor outcome associated with lamin A/C-positive tumors may be reflective of a more stem-cell-like phenotype (Willis et al., 2008).

4.6.7 The effect of NIR on stem cells

NIR irradiation abruptly induced subcutaneous adipocytes on the panniculus carnosus and CD34-positive cells around the subcutaneous adipocytes (Tanaka et al., 2011b). Adipose-derived stem cells express CD34 in higher percentages than bone marrow-derived mesenchymal stem cells (Yoshimura et al., 2009). CD34-positive human adipose-derived stem cells have a greater replicative capacity compared to CD34-negative cells (Suga et al., 2009). These results suggest that NIR irradiation may enrich and stimulate CD34-positive adipose-derived stem cells to increase subcutaneous adipocytes on the panniculus carnosus. Optically, fatty tissue can scatter NIR (Srinivasan et al., 2003), and fatty acids are the major NIR absorbing materials in soft tissues (Tsai et al., 2001). The oil in the liquid phase is transparent, whereas the oil in the solid phase is highly scattering to NIR (Van et al., 2005). The long-lasting induction of subcutaneous adipocytes may protect the underlying tissues, including the panniculus carnosus, against NIR damage.

NIR irradiation that simulated solar radiation non-thermally affected the subcutaneous tissues, cortical bone, and bone marrow (Tanaka et al., 2011b). The apoptotic damage to bone marrow cells might be minimized by a biological defense against NIR irradiation by means of an increase in subcutaneous and bone marrow adipocytes as well as cortical bone mass through the enrichment of CD34-positive stem cells at the inner surface of the bone cortex.

Lamin A and pre-lamin A regulate stem cell maintenance and differentiation by influencing key signaling pathways in stem cells (Prokocimer et al., 2009). Lamin A/C expression seems to be reduced or absent in undifferentiated or proliferative cells, but is observed in differentiated or non-proliferative cells, such as quiescent adult stem cells (Pekovic, 2008). Lamin A regulates stem cell maintenance through a range of regenerative signaling pathways, which suggests that the regulation of adult stem cell ageing may occur at a number of different pathway steps that intersect with lamin A, including adult stem cells, their progenitors, and/or stem cell niches (Pekovic, 2008). These results suggest that NIR radiation may stimulate stem cells, including cancer stem cells.

5. Conclusion

This simple technique of NIR irradiation might have a potential application for the transient mass reduction of melanoma before surgery, since the schedule reduces discomfort and side effects, reaches the deep subcutaneous tissues, and facilitates repeated irradiations.
In contrast, solar NIR radiation may also cause unexpected muscle thinning and stimulation of stem cells, including cancer stem cells, in areas of the body that are exposed to the sun. Therefore, exposed skin should be protected with sunscreens that block not only UV, but also NIR radiation, in order to prevent overlying skin ptosis, ageing, and oncogenicity. Additional non-thermal studies are required to decipher the effects on melanoma induced by both UV and NIR in humans.

6. Acknowledgements

We thank Ikuo Matsuyama for histological staining.

7. References

Ananthaswamy HN, Loughlin SM, Cox P, Evans RL, Ullrich SE, Kripke ML. (1997). Sunlight and skin cancer: Inhibition of p53 mutations in UV-irradiated mouse skin by sunscreens. *Nature Med.*3, 510-4.

Anderson RR, Parrish JA. (1981). The optics of human skin. *J Invest Dermatol* 77: 13-9.

Arimura T, Helbling-Leclerc A, Massart C, et al. (2005) Mouse model carrying H222P-Lmna mutation develops muscular dystrophy and dilated cardiomyopathy similar to human striated muscle laminopathies. *Hum Mol Genet.* 14, 155–69.

Arrington JH III, Lockman DS. (1979). Thermal keratoses and squamous cell carcinoma in situ associated with erythema ab igne. *Arch Dermatol.* 115: 1226–8.

Bain JA, Rusch HP, Kline BE. (1943). The effect of temperature upon ultraviolet carcinogenesis with wavelength 2,800–3,400A˚. *Cancer Res.* 3: 610–12.

Bakay M, Wang Z, Melcon G, et al. (2006) Nuclear envelope dystrophies show a transcriptional fingerprint suggesting disruption of Rb-MyoD pathways in muscle regeneration. *Brain.* 129, 996–1013.

Bäumler W, Abels C, Karrer S, Weiss T, Messmann H, Landthaler M, Szeimies RM. (1999). Photo-oxidative killing of human colonic cancer cells using indocyanine green and infrared light. *Br J Cancer.* 80(3-4):360-3.

Bergo MO, Gavino B, Ross J, Schmidt WK, Hong C, Kendall LV, Mohr A, Meta M, Genant H, Jiang Y, Wisner ER, Van Bruggen N, Carano RA, Michaelis S, Griffey SM, Young SG. (2002). Zmpste24 deficiency in mice causes spontaneous bone fractures, muscle weakness, and a prelamin A processing defect. *Proc Natl Acad Sci USA.* 99:13049–54.

Bliss J, Ford D, Swerdlow A, Armstrong B, Cristofolini M, Elwood J, Green A, Holly E, Mack T, MacKie R. (1995). Risk of cutaneous melanoma associated with pigmentation characteristics and freckling: systematic overview of 10 case-control studies. The International Melanoma Analysis Group (IMAGE). *Int J Cancer*. 62 (4): 367–76.

Broers JL, Ramaekers FC, Bonne G, Yaou RB, Hutchison CJ. (2006). Nuclear lamins: laminopathies and their role in premature ageing. *Physiol Rev.* 86(3):967-1008.

Busetti A, Soncin M, Jori G, Kenney ME, Rodgers MA. (1998). Treatment of malignant melanoma by high-peak-power 1064 nm irradiation followed by photodynamic therapy. *Photochem Photobiol.* 68: 377–81.

Danno K, Horio T, Imamura S. (1992). Infrared radiation suppresses ultraviolet B-induced sunburn-cell formation. *Arch Dermatol Res.* 284: 92–94.

Danno K, Mori N,Toda K, Kobayashi T, Utani A. (2001). Near-infrared irradiation stimulates cutaneous wound repair: laboratory experiments on possible mechanisms. *Photodermatol Photoimmunol Photomed*.17:261-5.

Davenport SA, Gollnick DA, Levernier M, Spooner GJR. (2006). Method and system for treatment of post-partum abdominal skin redundancy or laxity. United States Patent 20060052847. Available at: http://www.freepatentsonline.com/y2006/0052847.html

Dees C, Harkins J, Petersen MG, Fisher WG, Wachter EA. (2002) Treatment of murine cutaneous melanoma with near infrared light. *Photochem Photobiol.* 75: 296-301.

Dewey WC. (1994). Arrhenius relationships from the molecule and cell to clinic. *Int J Hyperthermia.* 10: 457–83.

Dey P. (2009). Nuclear margin irregularity and cancer: a review. *Anal Quant Cytol Histol.* 31(5):345-52.

Dougherty TJ, Gomer CJ, Henderson BW, Jori G, Kessel D, Korbelik M, Moan J, Peng Q. (1998). Photodynamic therapy. *J Natl Cancer Inst.* 90: 889–905.

Dover, J.S., Phillips, T.J. & Arndt, K.A. (1989). Cutaneous effects and therapeutic uses of heat with emphasis on infrared radiation. *J. Am. Acad. Dermatol*. 20, 278-86.

Ferrari M, Mottola L, Quaresima V. (2004). Principles, techniques, and limitation of near infrared spectroscopy. *Can J Appl Physiol.* 29(4):463-87.

Findlayson GR, Sams WM Jr, Smith JG. (1966). Erythema ab igne. A histopathological study. *J Invest Dermatol.* 46:104–7.

Foster CR, Przyborski SA, Wilson RG, Hutchison CJ. (2010). Lamins as cancer biomarkers. *Biochem Soc Trans.* 38:297-300.

Frank S, Oliver L, Lebreton-De Coster C, Moreau C, Lecabellec MT, Michel L, Vallette FM, Dubertret L, Coulomb B. (2004). Infrared radiation affects the mitochondrial pathway of apoptosis in human fibroblasts. *J. Invest. Dermatol*. 123:823-31.

Gates DM. (1966). Spectral distribution of solar radiation at the earth's surface. *Science*. 151:523-9.

Gerace L, Blobel G. (1980). The nuclear envelope lamina is reversibly depolymerised during mitosis. *Cell.* 19:277-87.

Goldberg DJ, Hussain M, Fazeli A, Berlin AL. (2007). Treatment of skin laxity of the lower face and neck in older individuals with a broad spectrum infrared light device. *J Cosmet Laser Ther*. 9:35-40.

Guinot C, Malvy DJ, Ambroisine L, Latreille J, Mauger E, Tenenhaus M, Morizot F, Lopez S, Le Fur I, Tschachler E. (2002). Relative contribution of intrinsic vs. extrinsic factors to skin aging as determined by a validated skin age score. *Arch Dermatol*. 138:1454-60.

Hewitt JB, Sherif A, Kerr KM, Stankler L. (1993). Merkel cell and squamous-cell carcinomas arising in erythema ab igne. *Br J Dermatol.* 128: 591–2.

Horwitz LR, Burke TJ, Carnegie D. (1999). Augmentation of wound healing using monochromatic infrared energy. Exploration of a new technology for wound management. *Adv Wound Care*. 12(1):35-40.

Hutchison CJ, Worman HJ. (2004). A-type lamins: guardians of the soma? *Nat Cell Biol* 6, 1062–7.

Jones CS, Tyring SK, Lee PC, Fine JD. (1988). Development of neuroendocrine (Merkel cell) carcinoma mixed with squamous-cell carcinoma in erythema ab igne. *Arch Dermatol*. 124: 110–3.

Karu T, Pyatibrat L, Kalendo G. (1994). Irradiation with He-Ne laser can influence the cytotoxic response of HeLa cells to ionizing radiation. *Int J Radiat Biol* 65: 691-7.

Karu T. (1999) Invited Review. Primary and secondary mechanisms of action of visible to near-IR radiation on cells. *J Photochem Photobiol B: Biol* 49: 1-17.

Kelleher DK, Thews O, Rzeznik J, Scherz A, Salomon Y, Vaupel P. (1999). Hot topic. Water-filtered infrared-A radiation: a novel technique for localized hyperthermia in combination with bacteriochlorophyll-based photodynamic therapy. *Int J Hyperthermia*. 15:467-74.

Kim MS, Kim YK, Cho KH, Chung JH. (2006). Infrared exposure induces an angiogenic switch in human skin that is partially mediated by heat. *Br J Dermatol*.155, 1131-8.

Kligman LH. (1982). Intensification of ultraviolet-induced dermal damage by infrared radiation. *Arch. Dermatol. Res.* 272, 229-38.

Kligman LH & Kligman AM. (1984). Reflections on heat. *Br. J. Dermatol*.110, 369-75.

Knize DM. (1996). An anatomically based study of the mechanism of the eyebrow ptosis. *Plast Reconstr Surg*. 97:1321-33.

Kochevar IE, Pathak MA, Parrish JA. (1999). Photophysics, photochemistry and photobiology. In: Freedberg IM, Eisen AZ, Wolff K, et al, eds. *Fitzpatrick's Dermatology in General Medicine*. New York: McGraw-Hill:220-9.Gates DM. (1966). Spectral distribution of solar radiation at the earth's surface. *Science*.151:523-9.

Kujawa J, Zavodnik IB, Lapshina A, Labieniec M, Bryszewska M. (2004). Cell survival, DNA, and protein damage in B14 cells under low-intensity near-infrared (810nm) laser irradiation. *Photomed Laser Surg*. 22: 504-8.

Liu J, Lee KK, Segura-Totten M, Neufeld E, Wilson KL, Gruenbaum Y. (2003). MAN1 and emerin have overlapping function(s) essential for chromosome segregation and cell division in Caenorhabditis elegans. *Proc Natl Acad Sci USA*. 15;100(8):4598-603.

Lobel J, MacDonald IJ, Ciesielski MJ, Barone T, Potter WR, Pollina J, Plunkett RJ, Fenstermaker RA, Dougherty TJ. (2001). 2-(1-hexyloxyethyl)-2-devinylpyropheophorbide-a (HPPH) in a nude rat glioma model: implications for photodynamic therapy. *Lasers Surg Med*. 29: 397–405.

Menezes S, Coulomb B, Lebreton C, Dubertret L. (1998). Non-coherent near infrared radiation protects normal human dermal fibroblasts from solar ultraviolet toxicity. *J. Invest. Dermatol*. 111;629-633.

Mounkes LC, Kozlov S, Hernandez L, Sullivan T, Stewart CL. (2003). A progeroid syndrome in mice is caused by defects in A-type lamins. *Nature*. 423, 298–301.

Mounkes LC, Stewart CL. (2004). Aging and nuclear organization: lamins and progeria. *Curr Opin Cell Biol* 16, 322–27.

Nagashima H, Hanada K, Hashimoto I. (1999). Correlation of skin phototype with facial wrinkle formation. *Photo Photodermatol Photoimmunol Photomed*. 15:2-6.

Nancini DM, Bolinger L, Li H, Kendrick K, Chance B, Wilson JR. (1994). Validation of near-infrared spectroscopy in humans. *J Appl Physiol*. 77:2740-7.

Nevskaya NA, Chirgadze YN. (1976). Infrared spectra and resonance interactions of amide-I and II vibrations of alpha-helix. *Biopolymers*. 15(4):637-48.

Newport JW, Wilson KL, Dunphy WG. (1990). A lamin-independent pathway for nuclear envelope assembly. *J Cell Biol*. 111(6):2247-59.

Niechajev I. (2004). Transpalpebral browpexy. *Plast Reconstr Surg*. 113:2172-80.

Nigg EA. (1992). Assembly and cell cycle dynamics of the nuclear lamina. *Semin Cell Biol.* 3(4):245-53. Odunze M, Rosenberg DS, Few JW. (2008). Periorbital aging and ethnic considerations: A focus on leteral canthal complex. *Plast Reconstr Surg.*121:1002-8.

Orenstein A, Kostenich G, Kopolovic Y, Babushkina T, Malik Z. (1999). Enhancement of ALA-PDT damage by IR-induced hyperthermia on a colon carcinoma model. *Photochem Photobiol.* 69(6):703-7.

Pekovic V, Harborth J, Broers JL, et al. (2007). Nucleoplasmic LAP2alpha-lamin A complexes are required to maintain a proliferative state in human fibroblasts. *J Cell Biol.* 176, 163–72.

Pendas AM, Zhou Z, Cadiñanos J, Freije JM, Wang J, Hultenby K, Astudillo A, Wernerson A, Rodríguez F, Tryggvason K, López-Otín C. (2002). Defective prelamin A processing and muscular and adipocyte alterations in Zmpste24 metalloproteinase-deficient mice. *Nat Genet.* 31:94–9.

Peter M, Nakagawa J, Dorée M, Labbé JC, Nigg EA. (1990). In vitro disassembly of the nuclear lamina and M phase-specific phosphorylation of lamins by cdc2 kinase. *Cell*. 61(4):591-602.

Prokocimer M, Davidovich M, Nissim-Rafinia M, Wiesel-Motiuk N, Bar DZ, Barkan R, Meshorer E, Gruenbaum Y. (2009). Nuclear lamins: key regulators of nuclear structure and activities. *J Cell Mol Med.* 13(6):1059-85.

Przyborski SA, Wilson RG and Hutchison CJ. Lamins as cancer biomarkers. (2010). *Biochem. Soc. Trans.* 38:297-300.

Pujol JA, Lecha M. (1993). Photoprotection in the infrared radiation range. *Photodermatol Photoimmunol Photomed.* 9:275-278.

Rawlings AV. (2006) Ethnic skin types: are there differences in skin structure and function? Review article. *Int J Cosmet Sci.* 28:79-93.

Reddy KL, Zullo JM, Bertolino E, Singh H. (2008). Transcriptional repression mediated by repositioning of genes to the nuclear lamina. *Nature.* 13;452(7184):243-7.

Santana-Blank LA, Rodriguez-Santana E, Vargas F, Reyes H, Fernández-Andrade P, Rukos S, Santana-Rodríguez KE. (2002). Phase I trial of an infrared pulsed laser device in patients with advanced neoplasias. *Clin Cancer Res.* 8: 3082–91.

Schieke SM, Schroeder P, Krutmann J. (2003). Review article. Cutaneous effects of infrared radiation: from clinical observations to molecular response mechanisms. *Photodermatol Photoimmunol Photomed.* 19: 228-234.

Schramm JM, Warner D, Hardesty RA, Oberg KC. (2003). A unique combination of infrared and microwave radiation accelerates wound healing. *Plast Reconstr Surg*. 111(1):258-66.

Schroeder P, Lademann J, Darvin ME, Stege H, Marks C, Bruhnke S, Krutmann J. (2008). Infared radiation-induced matrix metalloproteinase in human skin: Implications for protection. *J Invest Dermatol.* 128:2491-7.

Smith ED, Kudlow BA, Frock RL, Kennedy BK. (2005).A-type nuclear lamins, progerias and other degenerative disorders. *Mech Ageing Dev.* 126(4):447-60.

Spann TP, Goldman AE, Wang C, Huang S, Goldman RD. (2002). Alteration of nuclear lamin organization inhibits RNA polymerase II-dependent transcription. *J Cell Biol.* 18;156(4):603-8.

Srinivasan S, Pogue BW, Jiang S, Dehghani H, Kogel C, Soho S, Gibson JJ, Tosteson TD, Poplack SP, Paulsen DK. (2003). Interpreting hemoglobin and water concentration,

oxygen saturation, and scattering measured *in vivo* by near-infrared breast tomography. *Proc Natl Acad Sci U S A*. 100: 12349–54.

Stuurman N, Heins S, Aebi U. (1998). Nuclear lamins: their structure, assembly, and interactions. *J Struct Biol.* 122(1-2):42-66.

Suga H, Matsumoto D, Eto H, Inoue K, Aoi N, Kato H, Araki J, Yoshimura K. (2009). Functional implications of CD34 expression in human adipose derived stem/progenitor cells. *Stem Cells Dev.* 18:1201-9.

Sullivan T, Escalante-Alcalde D, Bhatt H, Anver M, Bhat N, Nagashima K, Stewart CL, Burke B. (1999). Loss of A-type lamin expression compromises nuclear envelope integrity leading to muscular dystrophy. *J Cell Biol.* 147(5):913-20.

Tafur J, Mills PJ. (2008). Low-intensity light therapy: exploring the role of redox mechanisms. *Photomed Laser Surg.* 26: 321-326.

Tanaka Y, Matsuo K. (2008). Protective agent against damage of biological tissue caused by near-infrared ray and product comprising the same. PCT/JP2008/063558, US2010/0129426 A1.

Tanaka Y, Matsuo K, Yuzuriha S, Shinohara H. (2009a). Differential long-term stimulation of type I versus type III collagen after infrared irradiation. *Dermatol Surg.* 35:1099-104.

Tanaka Y, Matsuo K, Yuzuriha S. (2009b). Long-term evaluation of collagen and elastin following infrared (1100 to 1800 nm) irradiation. *J Drugs Dermatol.* 8:708-12.

Tanaka Y, Matsuo K, Yuzuriha S. (2010a) Long-Term Histological Comparison between Near-Infrared Irradiated Skin and Scar Tissues. *J Clin Cosmet Invest Dermatol.* 3:143-49.

Tanaka Y, Matsuo K, Yuzuriha S, Yan H, Nakayama J. (2010b). Non-thermal cytocidal effect of infrared irradiation on cultured cancer cells using specialized device. *Cancer Science.* 101:1396-402.

Tanaka Y, Matsuo K, Yuzuriha S. (2010c). Long-lasting muscle thinning induced by infrared irradiation specialized with wavelength and contact cooling: A preliminary report. *ePlasty.* 10:e40.

Tanaka Y, Matsuo K, Yuzuriha S. (2011a).Long-lasting relaxation of corrugator supercilii muscle contraction induced by near infrared irradiation. *ePlasty.* 11:e6.

Tanaka Y, Matsuo K, Yuzuriha S. (2011b). Near-Infrared Irradiation Non-thermally affects Subcutaneous Adipocytes and Bone. *ePlasty.* 11:e12.

Tanaka Y, Matsuo K, Yuzuriha S. (2011c). Near-Infrared Irradiation Non-thermally Induces Long-lasting Vasodilation by Causing Apoptosis of Vascular Smooth Muscle Cells. *ePlasty.* 11:e22.

Tirlapur UK, König K. (2001). Femtosecond near-infrared laser pulse induced strand breaks in mammalian cells. *Cell Mol Biol.* 47: 131-4.

Travers JB, Edenberg HJ, Zhang Q, Al-Hassani M, Yi Q, Baskaran S, Konger RL. (2008). Augmentation of UVB radiation-mediated early gene expression by the epidermal platelet-activating factor receptor. *J. Invest. Dermatol.* 1284:55-60.

Tsai CH, Chen JC, Wang WJ. (2001). Near-infrared absorption property of biological soft tissue constituents. *J Med Biol Eng.* 21:7-14.

Tsukahara T, Fujimura T, Yoshida Y, Kitahara T, Hotta M, Moriwaki S, Witt PS, Simion FA, Takema Y. (2004). Comparison of age-related changes in wrinkling and sagging of the skin in Caucasian females and in Japanese females. *J Cosmet Sci.* 55:373-85.

Varga R, Eriksson M, Erdos MR, Olive M, Harten I, Kolodgie F, Capell BC, Cheng J, Faddah D, Perkins S, Avallone H, San H, Qu X, Ganesh S, Gordon LB, Virmani R, Wight

TN, Nabel EG, Collins FS. (2006). Progressive vascular smooth muscle cell defects in a mouse model of Hutchinson-Gilford progeria syndrome. *Proc Natl Acad Sci USA*. 103:3250–5.

Van Veen RL, Sterenborg HJ, Pifferi A, Torricelli A, Chikoidze E, Cubeddu R. (2005). Determination of visible near-IR absorption coefficients of mammalian fat using time- and spatially resolved diffuse reflectance and transmission spectroscopy. *J Biomed Opt*. 10:054004.

Venables RS, McLean S, Luny D, Moteleb E, Morley S, Quinlan RA, Lane EB, Hutchison CJ. (2001). Expression of individual lamins in basal cell carcinomas of the skin. *Br J Cancer*. 84(4):512-9.

Vogelstein B, Kinzler KW. (2004). Cancer genes and the pathways they control. *Nat Med*. 10:789-99.

Weyer LG. (1985). Near-infrared spectroscopy of organic substances. *Appl Spectrosc Rev*. 21:1-43.

Willis ND, Wilson RG, Hutchison CJ. (2008). Lamin A: a putative colonic epithelial stem cell biomarker which identifies colorectal tumours with a more aggressive phenotype. *Biochem Soc Trans*. 36:1350-3.

Wolf P, Donawho CK, Kripke ML. (1994). Effect of Sunscreens on UV radiation-induced enhancements of melanoma in mice. *J. Nat. Cancer. Inst.* 86 (2): 99–105.

Wust P, Hildebrandt B, Sreenivasa G, Rau B, Gellermann J, Riess H, Felix R, Schlag PM. (2002). Review article. Hyperthermia in combined treatment of cancer. *Lancet Oncol*. 3: 487–97.

Yang L, Guan T, Gerace L. (1997). Integral membrane proteins of the nuclear envelope are dispersed throughout the endoplasmic reticulum during mitosis. *J Cell Biol*. 137(6):1199-210.

Yang SH, Bergo MO, Toth JI, Qiao X, Hu Y, Sandoval S, Meta M, Bendale P, Gelb MH, Young SG, Fong LG. (2005). Blocking protein fornesyltransferase improves nuclear blebbing in mouse fibroblasts with a targeted Hutchinson-Gilford progeria syndrome mutation. *Proc Natl Acad Sci USA*. 102:10291–6.

Yoshimura K, Suga H, Eto H. (2009). Adipose derived stem/progenitor cells; roles in adipose tissue remodeling and potential use for soft tissue augumentation. *Regen Med*. 4:265-73.

Zaremba-Czogalla M, Dubińska-Magiera M, Rzepecki R. (2011). Laminopathies: the molecular background of the disease and the prospects for its treatment. Cell Mol Biol Lett. 16(1):114-48.

Zink D, Fisher AH, Nickerson JA. (2004). Nuclear structure in cancer cells. *Nat Rev Cancer*. 4:677-87.

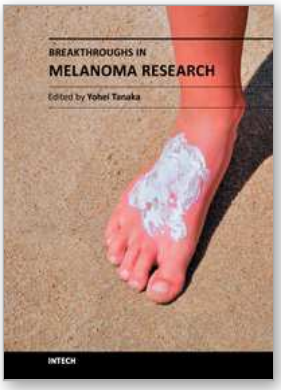

Breakthroughs in Melanoma Research

Edited by Dr Yohei Tanaka

ISBN 978-953-307-291-3
Hard cover, 628 pages
Publisher InTech
Published online 30, June, 2011
Published in print edition June, 2011

Melanoma is considered to be one of the most aggressive forms of skin neoplasms. Despite aggressive researches towards finding treatments, no effective therapy exists to inhibit the metastatic spread of malignant melanoma. The 5-year survival rate of metastatic melanoma is still significantly low, and there has been an earnest need to develop more effective therapies with greater anti-melanoma activity. Through the accomplishment of over 100 distinguished and respected researchers from 19 different countries, this book covers a wide range of aspects from various standpoints and issues related to melanoma. These include the biology of melanoma, pigmentations, pathways, receptors and diagnosis, and the latest treatments and therapies to make potential new therapies. Not only will this be beneficial for readers, but it will also contribute to scientists making further breakthroughs in melanoma research.

How to reference

In order to correctly reference this scholarly work, feel free to copy and paste the following:

Yohei Tanaka and Kiyoshi Matsuo (2011). Non-Thermal Effects of Near-Infrared Irradiation on Melanoma, Breakthroughs in Melanoma Research, Dr Yohei Tanaka (Ed.), ISBN: 978-953-307-291-3, InTech, Available from: http://www.intechopen.com/books/breakthroughs-in-melanoma-research/non-thermal-effects-of-near-infrared-irradiation-on-melanoma

INTECH
open science | open minds

InTech Europe
University Campus STeP Ri
Slavka Krautzeka 83/A
51000 Rijeka, Croatia
Phone: +385 (51) 770 447
Fax: +385 (51) 686 166
www.intechopen.com

InTech China
Unit 405, Office Block, Hotel Equatorial Shanghai
No.65, Yan An Road (West), Shanghai, 200040, China
中国上海市延安西路65号上海国际贵都大饭店办公楼405单元
Phone: +86-21-62489820
Fax: +86-21-62489821